Vibration Characterization and Active Vibration Control of Fully Clamped Thin Flexible Plate

by

Utku BOZ

A Thesis Submitted to the
Graduate School of Engineering
in Partial Fulfillment of the Requirements for
the Degree of

Master of Science
in
Mechanical Engineering

Koc University

September 2011
Koc University
Graduate School of Sciences and Engineering

This is to certify that I have examined this copy of a master's thesis by

Utku BOZ

and have found that it is complete and satisfactory in all respects,

and that any and all revisions required by the final

examining committee have been made.

Committee Members:

_____

Ipek Basdogan, Ph. D. (Advisor)

_____

Yaman Arkun, Ph. D.

_____

Cagatay Basdogan, Ph. D.

Date: _____

ABSTRACT

VIBRATION CHARACTERIZATION AND ACTIVE VIBRATION CONTROL OF FULLY CLAMPED FLEXIBLE PLATE USING PIEZOELECTRIC PATCH ACTUATORS

In this thesis, motivation is to investigate vibration behavior of the fully clamped thin flexible plate and suppress the vibration of this plate by applying active control methodologies. Active vibration control system is created using surface bonded piezoelectric patches as actuators and a Laser Doppler Vibrometer(LDV) as velocity sensor.

At the first part of this thesis, vibration characteristics of the fully clamped plate are investigated experimentally. Experimental modal analysis is completed using piezoelectric patches as actuators, and a laser Doppler vibrometer (LDV) as vibration sensor.

In the second part of the thesis, active vibration control of the fully clamped plate using velocity feedback algorithm is presented. Velocity feedback controller is implemented with an analog circuit. Undesired vibration and control actuation are created using piezoelectric patches and A LDV is recruited as velocity sensor. Three different piezoelectric patches are fixed on fully clamped plate and active vibration control performance with different configurations of those patches is analyzed. Besides active vibration control performance, effect of changing control gains of velocity feedback on the modal behavior of the plate is investigated.

Third part of this thesis presents results for active vibration control system designed using digital programmable controller. In this section, two different controller algorithms are utilized. First a proportional velocity feedback controller is designed and implemented.

For another analysis, preferred controller is state feedback controller. Using same set-up, and same equipments, controller performances on vibration suppression and effect of different controller gains on the plate for each digital controller case are analyzed. .

Keywords: vibration suppression, experimental modeling, piezoelectric patches, optimal control, velocity feedback control

ÖZET

HER TARAFI TUTTURULMUŞ ESNEK LEVHANIN PİEZOELEKTRİK YAMALAR ARACILIĞI İLE TİTREŞİM KARAKTERİZASYONU VE KONTROLÜ

Bu çalışmada amaç, dört tarafı tutturulmuş esnek bir levhanın titreşim karakterizasyonu ve aktif titreşim kontrolünün piezoelektrik yamalar kullanılarak başarılmasıdır. Aktif titreşim kontrolü için kullanılandüzenek, piezoelektrik yamalar ve Lazer Dopler Vibrometre (LDV) kullanılarak kurulmuştur. Piezoelektrik yamalar istenmeyen titreşimin ve kontrol sisteminin kaynağı olarak kullanılırken LDV ise hız sensörü olarak belirlenmiştir.

İlk kısımda sistemin karakteristiklerinin deneysel metodlar kullanılarak belirlenmesi anlatılmıştır. Deneysel mod analizi piezoelektrik yamalar ve LDV kullanılarak tamamlanmış; ve frekans cevap fonksiyonları(FRF) çıkarılarak sistemin titreşim karakteristiği analiz edilmiştir.

İkinci kısımda ise sistemin oransal hız geri besleme yöntemi ile titreşim kontrolü yapılmış ve sonuçlar gösterilmiştir. Kontrolcü analog bir devre yardımı kullanılarak tasarlanmıştır. İstenmeyen titreşimin kaynağı olarak kullanılan piezoelektrik yamaların oluşturduğu bozuntuLDV aracılığı ile algılanmış ve bu sinyal analog devreden geçirilerek kontrol amacı ile kullanılan piezoelektrik yamalara beslenmiştir. İlk üç titreşim modu için kontrol hedeflenmiş ve farklı piezoelektrik yama konfigürasyonları ile yapılan kontrol deneylerinin sonuçları sunulmuştur. Bunun yanı sıra, kontrolcünün sistem karakteristiğine etkisi farklı kontrolcü katsayıları için gösterilmiştir.

Üçüncü kısımda ise iki farklı kontrol metodu dijital ortamda tasarlanmış ve uygulanmıştır. Tercih edilen metodlar oransal hız geribeslemeli kontrolcü ve optimal kontrolcüdür. . Aynı deneysel düzenek kullanılarak gerçekleştirilenkontrolcü tasarımları ile aktif titreşim kontrolü hedeflenmiş ve başarılmıştır. İki kontrolcünün sisteme olan etkileri ve başarıları tartışılmış, daha detaylı bir araştırma için kontrolcü oranları değiştirilerek system karakteristiğindeki değişimler incelenmiştir. .

Anahtar Kelimeler: titreşim sönümleme, deneysel modelleme, piezoelektrik yamalar, optimal kontrol, hız geri beslemeli kontrol.

ACKNOWLEDGEMENTS

I gratefully thank my supervisor Assoc. Prof. Ipek Basdogan for her valuable support and wisdom. Her proficiency in vibration analysis and professional view on research guided me in the times that I think it is impossible to endure the difficulties. I also thank thesis comitee members Prof. Yaman Arkun and Assoc. Prof Çağatay Başdoğan for their valuable support and critical reading of my work.

I would like to thank Ugur Arıdoğan for his companionship and guidence. He taught me how to implement electronical components, use electronics and real life control design. Without his support things would be more complicated.

I thank my dearest for being in my life and support even when it is not possible to see each other.

I also thank Serkan Külah and Hakan Uçar for their friendship in vibration and acoustic laboratory. Without them the time other than my research study in lab would not be funny and productive.

I thank Engin Çukuroğlu, Talha Akyol and Başar Demir for their companionship and support as home mates. They helped me to create peaceful and funny off-work time in my home.

I also appreciate Gözde Kuşgöz, Güray Kuzu, Barış Çağlar, Fatma Virdil and Mehmet Ayyıldız for their valuable support in my hard times. I always knew that they are entrusted friends and secret keepers.

Without, Berkay Yarpuzlu, Reşit Haboğlu, Gökalp Gürsel and Arda Aytekin, my spare times in Koç universtiy would not be funny and motivating.

Finally I would like to appreciate my mother Ayten, my father Celaleddin and my sister Ukte. Their love, support and respect to my decisions, their guidance in love and their endeavours on shaping my personality led me to the position I am in now. I love you all and I owe my success to your presence.

TABLE OF CONTENTS

LIST OF FIGURES

LIST OF TABLES

CHAPTER 1

INTRODUCTION

1.1 Overview

The undesirable effects of mechanical vibrations such as significant structural deformations and failures, increase in power consumptions lead the engineers to investigate the vibration characteristics and attenuate vibration levels in engineering structures. In 1980s, the usages of large structures as the components of the space vehicles were resulted in new challenges in vibration control since these structures are lightly damped and have long decay times. Researchers were motivated to design and implement active vibration control to these lightly damped structures with piezoelectric materials. In one of the first research studies relevant to the usage of piezoelectric materials in active vibration control, Bailey and Hubbard[1] designed an active damper system by using piezoelectric material as distributed actuator for the vibration suppression of the cantilever beam. Subsequently, Crawley and Luis[2] developed and experimentally verified the analytical model of piezoelectric materials. The main contribution of this research work was the accurate prediction of performance and effectiveness of piezoelectric materials when they are used as actuators. The passive isolation techniques are not generally feasible and efficient for low frequency vibration suppression; instead, piezoelectric materials can be used to suppress the low frequency vibration. Ro and Baz[3] investigated the overall effectiveness of the active and passive treatments for vibration and sound attenuation. Their results revealed that active treatments such as bonded piezoelectric patch actuators can significantly reduce the vibration and sound radiation better than the passive treatments. Thereafter, development and commercial availability of piezoelectric elements enabled

them to be employed widely as actuators and sensors for active vibration attenuation of structures.

In the literature, there are published review articles discussing fundamental aspects of active vibration control. Rao and Sunar[4] published a review paper on employment of piezoelectric materials as sensors and actuators for control of flexible structures. In this review paper, they presented the general framework of structural control strategies and presented the applications in various fields. One of the most common application areas is aerospace industry, since the aerospace structures are flexible and have limited tolerance for vibration. The following review paper presented the key applications of smart structures in aeronautical applications with potential uses[5]. The authors categorized the smart materials in terms of their energy-exchange capabilities and also discussed the benefits of using smart structures in aeronautical applications.

Modeling and performance prediction of piezoelectric sensors and actuators as elements of smart structures is essential for building feasible and reliable vibration control systems. Chee et al.[6] presented the modeling approaches for piezoelectric materials. As discussed in their article, analytical and finite element modeling of piezoelectric materials with host structures can be built using the linear constitutive piezoelectric equations. This approach is reliable for low actuation authority, however for high actuation authority, different methodologies such as modeling of transverse actuation using analytical and finite element methods must be applied.

The choice of controller type and optimal positioning of sensors and actuators are important aspects of design and implementation of active vibration control systems. There are some published technical review papers discussing the controller algorithms and optimal placements. For instance, Alkhatib and Golnaraghi[7] reviewed the controller architectures and presented the general design procedures for the active vibration control systems. In this review paper, they stated the advantages and disadvantages of different

controller architectures with various application examples. For example, they stated that the active damping system is advantageous when the vibration suppression is performed around resonance frequencies. This active damping system ensures stability when collocated sensor and actuator pairs are used on the host structure.

In another study, Gupta et al.[8] concentrated on the optimal positioning investigations of piezoelectric sensors and actuators. In this technical review, the optimization techniques are presented and the results of former research studies are given. It is stated that investigation of optimal positioning in complex structures with complex boundary conditions is a growing research field since the optimization techniques are mostly applied to the placement of actuators and sensors on non-complex structures with simple boundary conditions.

For robust active vibration control systems, the structural modeling techniques and modeling of uncertainties are also important. A comprehensive methodology for design and validation of a robust controller is presented by Iorga et al.[9]. In this review paper, structural modeling techniques with uncertainty analysis is given and robust H_∞ design is conducted by placing emphasis on robust control concepts.

Meanwhile, the piezoelectric materials also attracted attention of the researchers working on noise control. In a review paper on smart structures and integrated systems, Chopra[10] stated that most of the applications for aerospace vehicles are focused on minimization of vibration levels; however, interior and exterior noise reduction using piezoelectric materials is also a potential research area for transport vehicles. Hanselka[11] named the use of smart materials in active noise and vibration control as innovative technology and gave an application example of active noise reduction. In this example, piezoelectric materials served as sensors and actuators to reduce structural-borne noise and the results showed that this application of technology is possible and advantageous.

Over the years, researchers focused on eliminating or reducing undesired vibrations. Vibration is reduced by means of active and passive methods. In the next section, an overview on active vibration control systems is presented.

1.2 Active Vibration Control

Suppressing vibration with externally induced excitations is a commonly used method for active vibration control. In this method, sensors and actuators are used to achieve control of the structure to decrease undesired vibration. Such methodology is called active vibration control.

Advances in signal processing technology and computers enabled researchers to be able to implement active vibration control on comlex structures[7]. In order to apply active vibration control, a mechanical structure is excited using an external disturbance source. Vibration of the structures are measured with sensors. Based on the transmitted sensor output, a control actuator is used to create a counter effect on the actuator location to suppress vibration. Currently, active vibration control methods are not robust enough for industrial applications. However, new advancements in active vibration control and smart materials will make it possible in the near future[12].

Different controller architectures are applied to achieve a succesfull active vibration control system. In the following section, an overview of controller algorithms for active vibration and noise control systems are presented.

1.2.1 Active Vibration Control Architectures

In general, the controllers are designed for two different tasks: tracking a trajectory or rejecting disturbances. For active vibration suppression systems, the task is the rejection of external disturbances and attenuation of vibration levels. These can be achieved via feedback and feedforward controllers. Feedback controllers use disturbance signals on the

sensor location to produce a control input. In feedforward control, major disturbance loads are measured and used to generate controller output. The generic block diagrams of these controller algorithms are presented in Figure1.1a and Figure1.1b. The advantages and disadvantages for those controllers are listed in Table1-1.

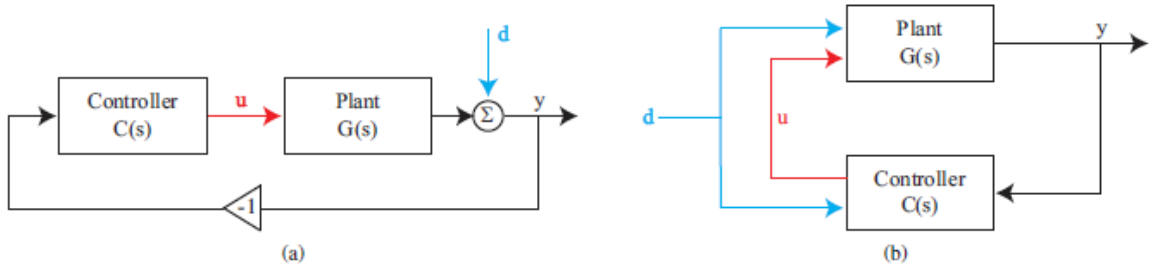

Figure 1.1 Generic Feedback and Feedforward Controller Block Diagrams: (a) Feedback Control (b) Feedforward Control

Feedback algorithms are divided to two general groups. Active damping systems and model based controller[13].Among active damping systems, proportional feedback control is widely used control architecture.

Proportional feedback control is simply to control a plant by feeding proportionally amplified error signal to a control actuator. Using a predefined sensor, error measurements on sensor location is acquired and processed. Processing of the error signal means to negatively error signal in magnitude and create a control signal. Next step is to transmit control signal to control actuator.

Different researchers used proportional feedback algorithms for vibration control applications. Fakhari et al numerically analyzed effectiveness of feedback control algorithms for functionally graded plates[14]. Okumura and his colleagues analyzed feedback control behavior of clamped plate numerically for surface bonded PZT patches [15].

Table 1-1 Advantages and Disadvantages of Control Algorithms on Active Vibration Control

Type of control	Advantage	Disadvantage
Feedback		
Active Damping	• Simple to implement • Does not require accurate model of plant • Guaranteed stability when sensors an actuators are collocated	• Effective only near resonance
Model Based(LQR,LQG,H_∞ ...)	• Global method • Requires accurate model of the plant • Attenuates all disturbance within the control band-with	• Limited bandwidth • Requires low delay for wide bandwidth • Spillover
Feedforward		
Adaptive filtering of reference(x-filtered LMS)	• No model is necessary • Robustto inaccuracies in plant estimate and to change in plant transfer functions • More effective for narrowband disturbance	• Reference/error signal is required • Local method and may amplify vibration somewhere else • Large amount of real-time computations

Model based feedback controllers utilize models created for the structures. Models for accurate system representation are created via different methods. Experimental modeling, theoretical modeling and finite element modeling(FEM) are possible methods. In experimental modeling a model is created using experimentally derived data. Besides experimental modeling, theoretical calculations utilizing lumped element method, Rayleigh Ritz method are used to understand behavior of plant. In addition to those, FEM is another

method. In FEM, structure is modeled as combination of substructures and utilizing relation between those substructures, general behavior of plant is modeled.

In model based controllers, model obtained using any of modeling methods is used for proper control application. Two different model based controllers are presented. Those are robust controllers and optimal controllers.

Optimal controller can be defined as the controller type that minimizes a cost function based on the required measure of the system's response. Linear Quadratic Regulator(LQR) is one of the widely used optimal controller and one optimal controller preferred for this study. In this controller scheme, current measured or observed states are fed back to the system after matrix multiplication of states with a predefined optimal gain matrix. For optimal gain matrix calculations, weights of the states and the inputs are tuning parameters for cost function minimization.

In literature, many researchers used LQR for vibration attenuation. Ryall analyzed effectiveness of optimally placed piezoceramic patches using optimal feedback control[16]. LQR algorithm is used numerically to overcome vibration in plate-like structures and applications of LQR can be found in [17-19].

Robust controllers concentrate on the tradeoffs between performance and stability in the presence of uncertainty in the system model as well as the exogenous inputs to which it is subjected[7]. LQG and H_∞ are well known controllers among such controller type.

LQG accounts for the disturbance cases that the system is affected and by minimizing optimal cost function with consideration of the characteristics of system uncertainties, achieves robust control. In literature many researchers utilized LQG in active vibration control. Chomette et al. proposed an LQG controller and demonstrated its effectiveness for PCB systems[20]. Hwang et al. demonstrated effectiveness of LQG controller and optimized the control locations[21]. Sanda and Takashi utilized LQG to suppress flutter of

aluminum wing plate[22]. Besides those researchers, different researchers also utilized LQG to show effectiveness of their controller design [23-26].

H_∞ is another robust controller used for suppressing vibration of structures. The aim of such robust controller is to minimize H_∞ norm of the transfer function between disturbances and output signal while considering internal stability of closed loop system. For effective and stable controller design, system uncertainties and performance criteria are included during the H_∞ controller design. However for stability assurance, design of the robust controller may be too conservative. For better performance of the controller, structured singular μ analysis is completed to analyze robustness and performance of the controller with parameters of uncertainty assumptions and weight selections. For H_∞ controller application to vibration control of the structures, Iorga et al addressed design considerations for robust H_∞ controller[9]. Besides concerns on design considerations, some numerical and experimental analyses are presented. For example, Jiang simulated effectiveness of H_∞ robust controller for decentralized configuration for the control of plate with parametric uncertainties[27]. In order to see more application examples related to H_∞ controller implementation for vibration control please refer to [28-32].

1.2.2 Sensors and Actuators

In this section, sensors and actuators used for active vibration control are presented. Since preferred actuator type for this thesis is piezoelectric materials, the scope of this section is limited with piezoelectric materials.

Piezoelectric materials have a recoverable strain of %0.1 under electrical field. Those materials can be used as sensors and actuators. Piezoelectric materials are divided to two major classes; Polymers and ceramics. Piezopolymers are recruited as sensors mostly since they require extremely high voltage and have limited control authority.Piezoceramics are used as both actuators and sensors. Piezoceramics are effective even in ultrasonic

applications and suit well for the applications with high precision even in nanometer range. The best known piezoelectric material is Lead Ziconate Titanate(PZT)[33].

Piezoelectric materials are started to be used in vibration control over 25 years ago. Bailey and Hubbard[1] designed a system to control vibration of cantilever beam. In time, new materials like PVDF and PZT are introduced and researchers utilized those materials for their applications. Piezoelectric materials are used in many research studies. Aoki et al[34] analyzed piezoelectric materials for velocity feedback control. Caruso et al simulated application of piezoelectric materials to suppress vibration of steel cantilevered plate[35]. Chellabi et al applied state feedback controller to plate structure utilizing piezoelectric materials[36]. Besides those studies, there are other simulation and experiment based vibration control analysis with piezoelectric materials [37-39].

Sensor measurements for vibration control can measure displacement, velocity, acceleration and/or strain. Displacements can be measured with inductive capacitive sensors and optical sensors. Capacitive and optical sensors have resolution in the nanometer range. Piezoelectric accelerometers are also very popular but they are not as efficient as the other sensors in measuring DC components[34]. Strains over surface can be measured with strain gages, piezoceramics, piezopolymers and fiberoptics. Those type of sensors can be embedded in the structure[33]. Laser doppler vibrometers are also used effectively for vibration control. Main advantage of using an LDV is preventing passive damping effect of the structural sensors [34].

1.3 Contribution of This Thesis

Considering all of the advancements in the previous studies, the main contribution of this thesis is to design and develop an active vibration control system to attenuate the vibration of a plate-like structure by employing surface-bonded piezoelectric patches as actuators and a collocated velocity sensor for vibration measurements. This study focuses on the comparison of two different control architectures and presents the results of vibration attenuation levels of these two methods. The following procedures are followed in developing the vibration control systems used in this study.

- The dynamics of the flexible plate is analyzed experimentally to investigate the vibration characteristics of the structure.
- Piezoelectric patches are used for actuating and exciting the structure
- LDV is used as the contactless velocity sensor.
- Proportional velocity feedback algorithm is used for vibration control and an analog circuit is built to implement the control scheme.
- A model based controller (optimal controller: LQR) is used as the second alternative for vibration control
- The performance of the two control architectures are compared

1.4 Outline

In chapter 2, Investigation of vibration characteristics of the fully clamped plate is presented with different piezoelectric patch configurations. In chapter 3, the implementation of a velocity feedback controller using an analog circuit is demonstrated. Various sensor/actuator locations are investigated and the effects of location on attenuating

different modes of the structure are presented. In chapter 4, vibration suppression of the smart plate with a digital controller implementation is presented. For this purpose, two feedback algorithms (velocity feedback and LQR) are designed and implemented. Performance of implemented algorithms is compared and changes in vibration characteristics of the smart plate due to the controller algorithm are analyzed. In Chapter 5, the discussion and conclusion of the thesis is given.

CHAPTER 2

SYSTEM CHARACTERIZATION

2.1 Introduction

In this chapter, vibration characterization of a fully clamped thin flexible plate is presented. Investigation of vibration characteristics of the fully clamped plate is completed with different piezoelectric patch configurations. Three different piezoelectric patches are bonded on the surface of the plate. Driving signal for the actuators is created with a data acquisition system and a Laser Doppler Vibrometer (LDV) is used as the vibration sensor. Frequency domain analysis of the system is completed for each configuration. Then the resultant behavior of the plate is investigated and analyzed separately for each configuration.

2.1.1 Smart Plate

For the rest of the thesis, the fully clamped plate is referred as “smart plate”. The smart plate is a steel plate with dimensions of 1000mm x 1000mm x 1.25mm with three surface bonded PI Duraact P876.A12 piezoelectric patches[40] (PZT, lead zirconate titanate) patches as shown in Figure 2.1. The piezoelectric patch model is shown in Figure2.2.

Figure 2.1 The Smart Plate

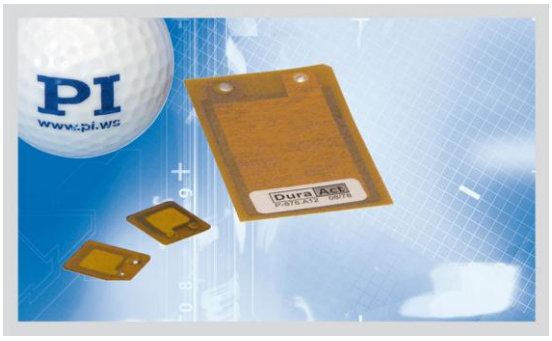

Figure 2.2 Duraact P876.A12 Piezoelectic Patch

Piezoelectric patches are bonded on the surface of the plate with superglue. The patch located at the center is called the center patch while, the one located on the left-upper

part of the plate is called northwest patch and third patch is called the southwest patch. Locations of these patches are shown in Figure2.3.

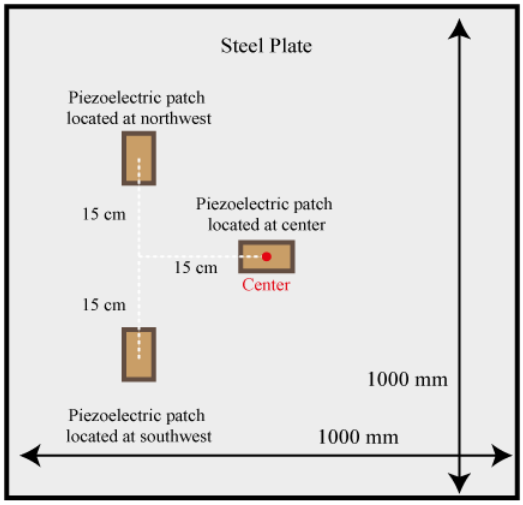

Figure 2.3 The Smart Plate with Surface Bonded Piezoelectric Patches

2.1.3 Investigation of Vibration Characteristics of the Smart Plate Using Piezoelectric Actuators

This section presents the vibration characteristics of the smart plate. In the first experiment, only northwest patch is activated and sensor location is chosen as northwest of the smart plate. In the second experiment, only center patch is used to excite the smart plate and sensor location is changed to center of the plate. In the final experiment, southwest piezoelectric patch is activated. Effectiveness of the southwest patch on the northwest of the plate is analyzed. Then, the center of the piezoelectric patch located at center is chosen as the sensor location and effect of southwest patch on this location is investigated. LDV[41] is used as the sensor for all of the experiments. Frequency domain analysis is

completed with NetDB[42] data acquisition system. In all configurations, a sine sweep signal with frequency components between 2-100 Hz is created to drive the piezoelectric patches. One analog output channel of NetDB system is used to generate the signal and it is transmitted to the piezoelectric patches via an amplifier E413.D2[43] supplied by PI Tech. Setting of the frequency domain analysis is tabulated in Table 2-1.

Table 2-1 Settings of the Frequency Domain Analysis

Signal Type	Sine Sweep
Frequency Component	2-100 Hz
Time for one cycle of signal	50 seconds
Sampling rate	51200 Hz
Block Size	4096
Frequency span	156 Hz
Duration of analysis	300 seconds
Average	57
Window type	Hanning
Overlap	50 %

Figure 2.4 shows the experimental setup for measuring the vibration characteristics of the smart plate. The same setup is used for the other experiments in this chapter. Only the sensor location and the active piezoelectric patches change for different configurations.

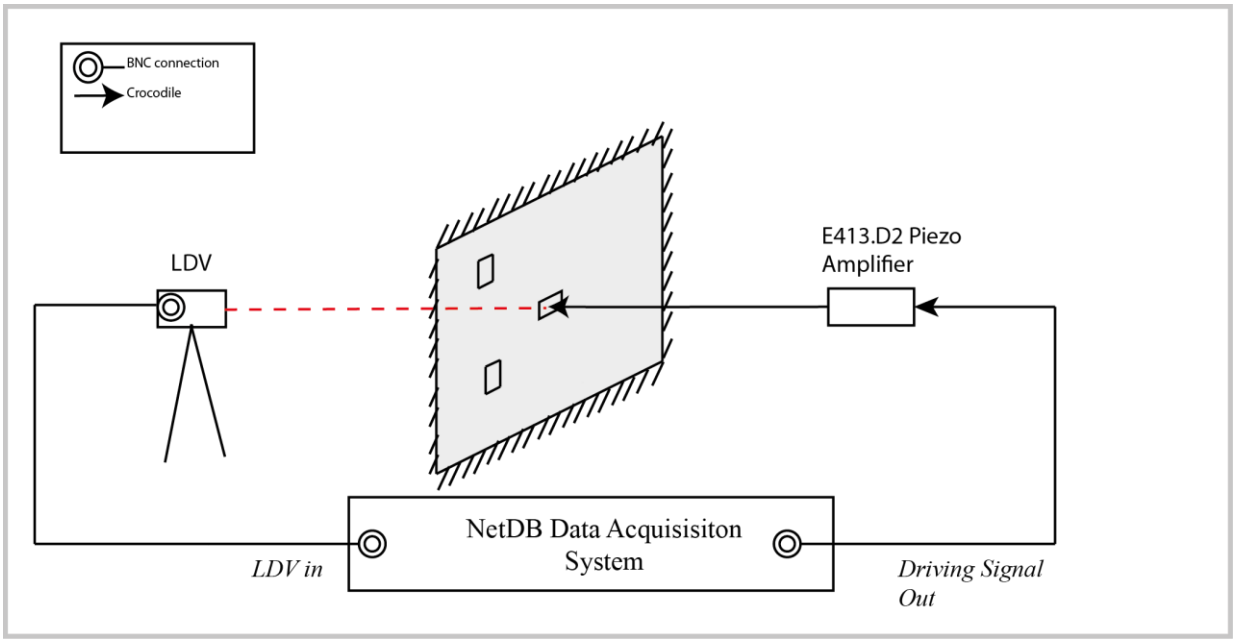

Figure 2.4 Experimental Setup for Vibration Characterization

2.1.3.1 Collocated Sensor-Actuator Pair at the Northwest Location

In this section, frequency response function (FRF) of the smart plate is obtained using a collocated sensor-actuator pair at the northwest location (see Figure 2.5).

As it can be observed from the figure, the first mode of the smart plate is at 13.57 Hz. The second mode is at 26.86 Hz and the third mode is at 30.18 Hz. Magnitudes of the frequency responses related to those frequencies are 73.09 dB, 77.21 dB and 69.44 dB respectively. In this configuration, first three modes can be observed since those modes can be excited by the northwest patch.

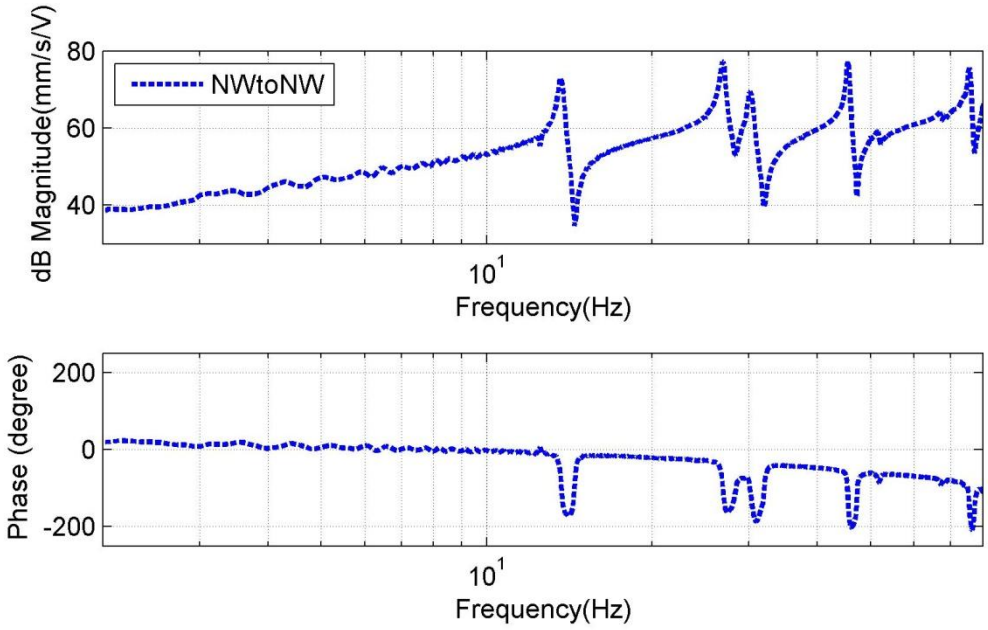

Figure 2.5 FRF of the smart plate (collacated sensor-actuator pair at the northwest location)

2.1.3.1 Collocated Sensor-Actuator Pair at the Center Location

In this section, frequency response function (FRF) of the smart plate is obtained using a collocated sensor-actuator pair at the northwest location (see Figure 2.6).

As it can be observed from the figure, the first mode of the smart plate is at 13.87 Hz. Magnitude of the frequency response at the first resonance frequency is 79.23 dB. The second and third modes of the plate cannot be observed when the plate is excited from the center since center is nodal for first mode. It is also observed that actuating the plate at the center is more effective when the first mode is considered.

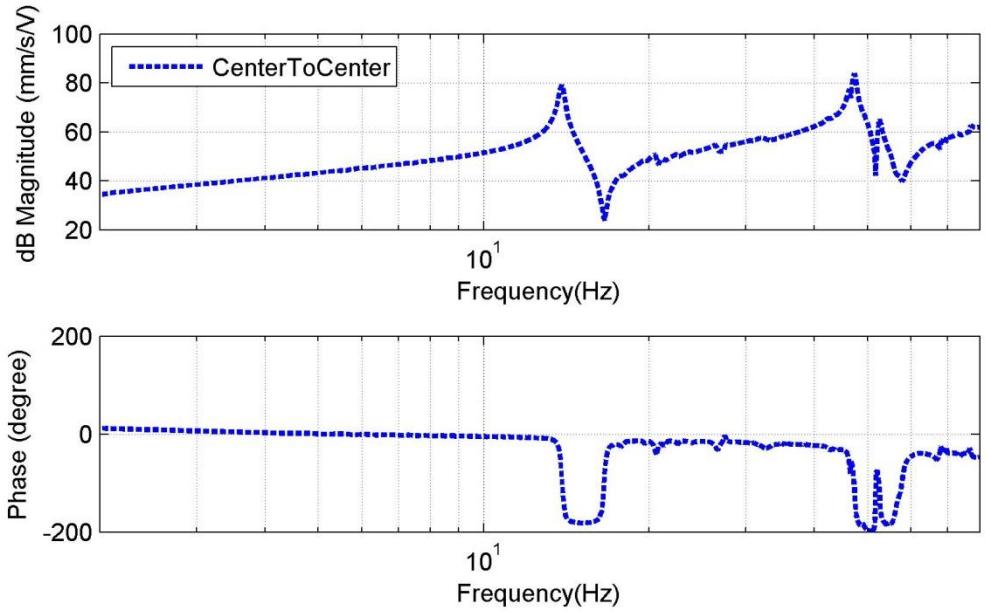

Figure 2.6 FRF of the Smart plate (Collacated Sensor-Actuator Pair at the Center Location)

2.1.3.2 Actuator at Southwest Location

In this section, frequency response function (FRF) of the smart plate is obtained using an actuator at the southwest location. Two different experiments are performed using the southwest patch. In the first configuration, sensor location is selected as collocated to the northwest patch(see Figure 2.7). In the second configuration, sensor location is moved to center of the smart plate (see Figure 2.8).

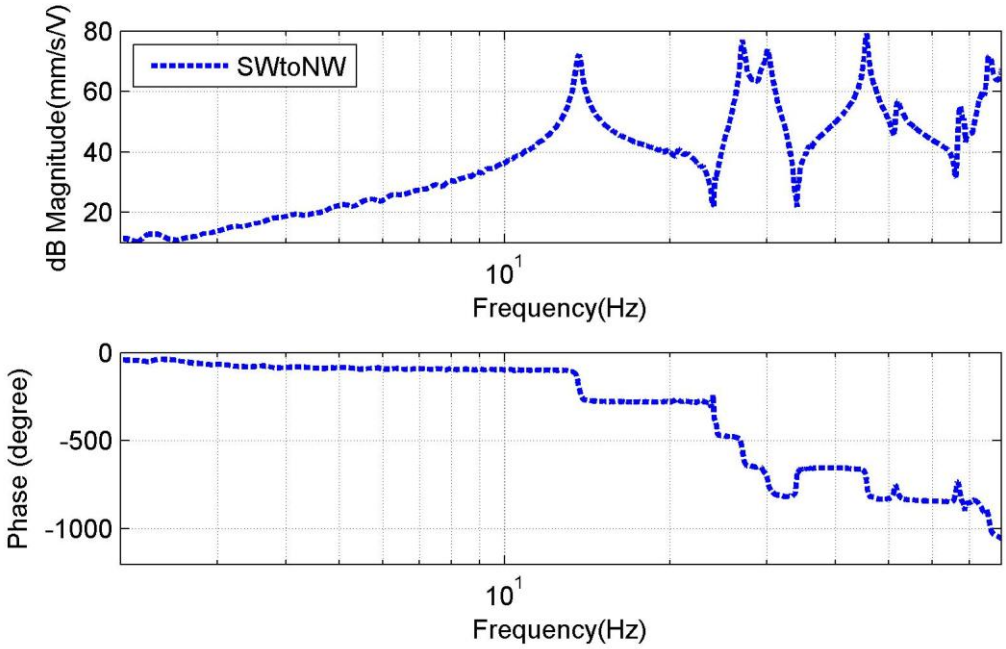

Figure 2.7 FRF of the Smart Plate (Actuator at Southwest, Sensor at Northwest

As it can be observed from Figure 2.7, the first mode is at 13.67 Hz. The second mode is at 27.05 HZ and third mode is at 30.08 Hz. At the first mode, response of the smart plate is 72.25 dB. For second and third modes, smart plate responds with magnitudes of 76.99 dB and 73.85 dB. It is obvious from the FRF that the southwest patch is capable of exciting first three modes the structure.

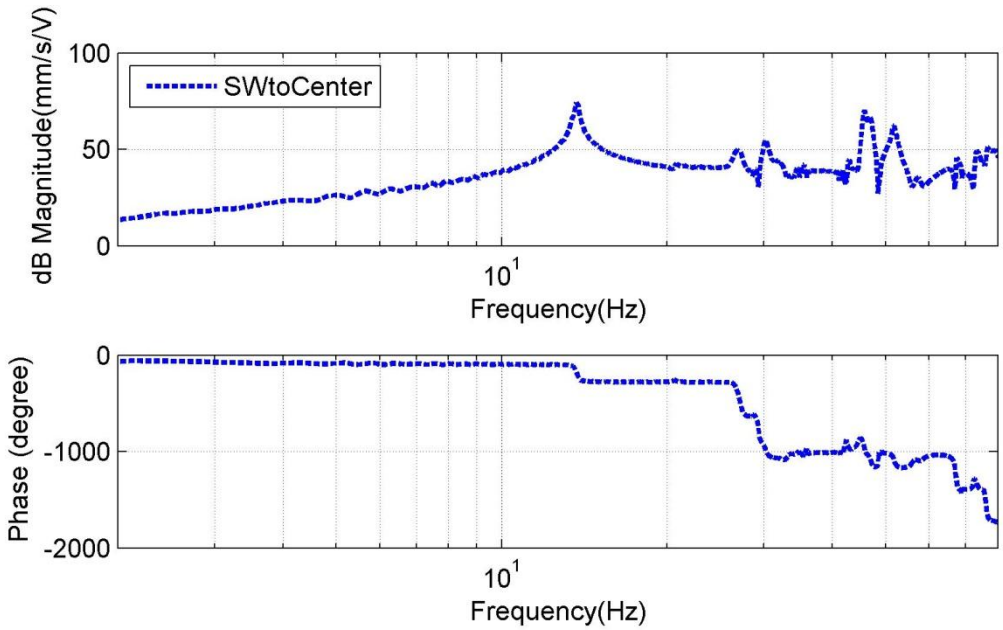

Figure 2.8 FRF of the Smart Plate (Actuator at Southwest, Sensor at Center)

As it can be observed from the figure, the first mode of the plate is at 13.67 Hz. The second mode is at 26.86 Hz and the third mode is at 30.18 Hz. Responses of the smart plate for those frequencies are 74.3 dB, 49.25 dB and 55dB.

2.2 Conclusion

In this chapter, frequency response functions of the smart plate with different sensor-actuator configurations are presented. In all cases, NetDB data acquisition system is used for frequency domain analysis and a LDV is used as the sensor.

It was observed that when the plate was excited at the center, it was very effective on the first mode of the plate. However, the second and third modes were not excited because

center location is a nodal point for those modes. The second and third modes were observed when the plate was excited at northwest or southwest locations.

CHAPTER 3

ANALOG VELOCITY FEEDBACK CONTROLLER FOR VIBRATION SUPPRESSION OF THE SMART PLATE

3.1 Introduction

In this chapter, an analog circuit is designed to implement proportional velocity feedback controller to suppress the vibrations of the smart plate. Vibration characterization studies of the smart plate presented in chapter 2 indicates that controller implementation to attenuate vibration is suitable using available sensors and actuators. For control system design southwest patch is used to create the disturbances on smart plate. A Laser Doppler Vibrometer (LDV) is used as sensor and the sensor data is transmitted to the analog circuitry. The acquired data is inverted and amplified to create controller output signal. This controller output signal is then applied to piezoelectric patches to suppress vibrations of the smart plate.

Two different configurations are analyzed for the system. In the first experiment, the plate is excited using southwest patch and center patch is used as the actuator to suppress vibration. Control gain yielding best controller performance is adjusted for first vibration mode of the smart plate. In this case, LDV is used to acquire data from the center location. Frequency and time domain analysis of the controller performance are completed. Effect of the controller on modal behavior of the smart plate is analyzed using three different control gains.

In the second configuration, northwest patch is used as the actuator for vibration suppression while the plate is still excited from the southwest location. For this experiment, LDV is used as the sensor to collect data at the northwest of the plate. Controller is tuned to yield best control performance for the first mode of the smart plate. Frequency and time domain analysis of the controller are completed to show effectiveness of the controller. Effect of the controller on modal behavior of the smart plate is analyzed using three different control gains.

3.2 Feedback Control Theory

Proportional feedback controller used in this study is presented in this chapter. In proportional feedback control, the aim is to minimize effect of disturbances on the system.

In the proportional feedback control, controller output signal is created by amplifying the output signal with a predefined gain. In Figure 3.1, block diagram of the closed loop control system of the proportional feedback controller is shown.

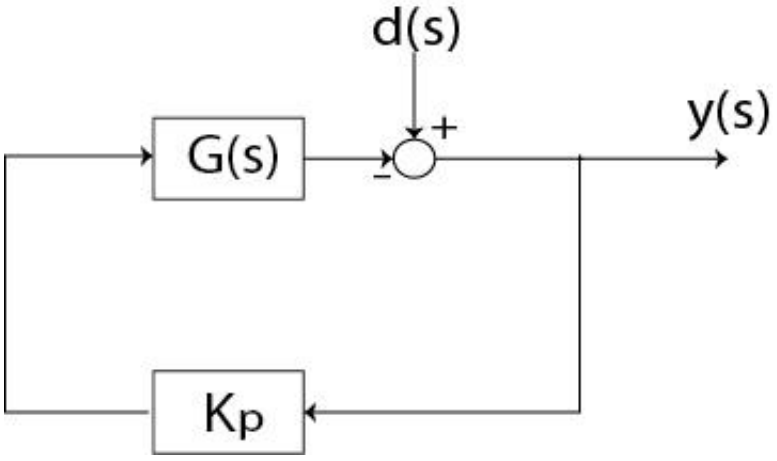

Figure 3.1 Block Diagram of Feedback Controller

The d(s) shown in block diagram is the disturbance source.Disturbance on the system generates undesired vibrations on the smart plate which is represented by y(s). In

proportional feedback controllers, a sensor is used to measure error. The sensor output,y(s), is acquired and transmitted to the controller. In the controller, the y(s) is multiplied by the predefined gain and the controller output signal is generated. The control actuator creates another counter vibration on the system to decrease effect of the original disturbance. Closed loop transfer function of the system plant is derived as follows.

$$d(s) - K_p G(s) y(s) = y(s) d(s) = y(s) + K_p G(s) y(s) \tag{3.1}$$

$$\frac{y(s)}{d(s)} = \frac{1}{1 + K_p G(s)} \tag{3.2}$$

Adjusting the gain changes the closed loop transfer function of the system so the response of the system can be minimized under the effect of the existing disturbance.

3.3. Proportional Velocity Feedback Controller Design

Proportional velocity feedback controller with collocated sensor and actuator pair provides active damping at the resonance frequencies of the structures. Infact, the proportional velocity feedback controller can be employed effectively in the lower-frequency modes of the structure, because of stability issue of the phase lag. In the high-frequencies, phase lag deteriorates the stability of the controller and the closed-loop system becomes unstable. This high-frequency stability problem can be eliminated by decreasing the proportional gain or including a low-pass filter in the closed-loop. Since only a feedback signal is amplified and fed back to the system, the delay and the computational cost is very low. It is possible to apply this control scheme using analog circuits since there is only one controller parameter and no need to calculate the variables like current states or to observe the behavior of plant with any algorithm.

During the tuning process of the controller, the proportional feedback gain is increased manually and the system response is observed. Gain leading to best performance for the first vibration mode of the smart plate is chosen as the controller gain. As previously indicated, phase lead/lag should be avoided for a stable controller. For this reason a low-pass filter is included in the control loop. Also it has been observed that the collocation of the sensor actuator pair guarantees stability[44]. The target of the LDV is collocated with piezoelectric patch actuator to have stable closed-loop system with proportional feedback control.

3.3.1 Implementation of the Controller

The designed proportional velocity feedback controller is implemented on a breadboard by using the circuit shown in Figure3.2. This analog circuit includes one inverting amplifier and low-pass filter. The measured sensor voltage signal (Vin) is passed through a low pass filter which is in the form of resistor-capacitor (RC) filter. The cut-off frequency of this filter equals to one divided by multiplication of resistor and capacitance value. The aim of this low-pass filter is the attenuation of high-frequency components of the sensor signal. After passing through this filter, the filtered signal is fed to the inverting amplifier. This inverting amplifier includes an operational amplifier (op-amp) and two resistors as indicated in Figure3.2. The op-amp is powered by dual polarity. The filtered sensor voltage is connected through input resistor R_c to the positive input channel of the op-amp. Then, a jumper resistor R_f is included between positive input channel and the output channel, whereas negative input channel is connected to the ground. By passing through this inverting amplifier, the sign of filtered sensor signal is inverted and its voltage value is amplified. The amplifier ratio is equivalent the ratio of jumper resistor R_f and input resistor R_c. Finally, this amplified and inverted signal serves as the proportional controller output signal.

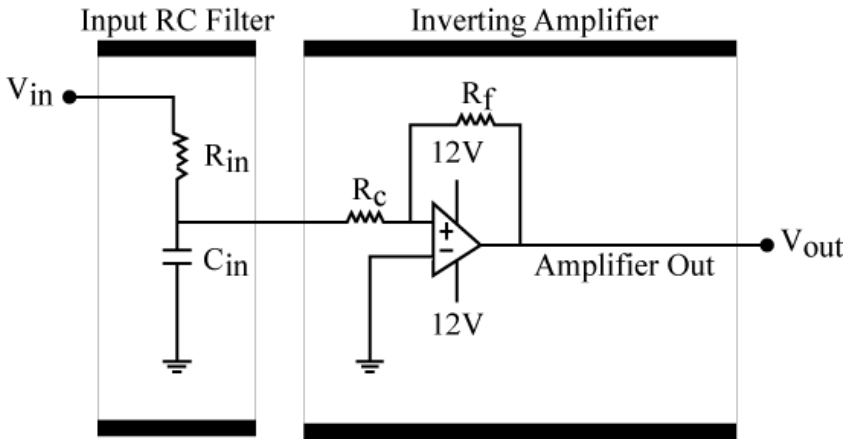

Figure 3.2 Implementation Diagram for Analog Proportional Velocity Feedback Controller

The amplified output voltage is then transmitted to piezoelectric patches for vibration attenuation. After designing the parameters, analog circuit is built. The amplifier is used as inverting amplifier. RC low pass filter is used as the analog filter. LM324N model type op-amp is used. It must be supplied with DC voltage and it is used as dual polarity op-amp circuit. Input voltage given to op-amp is 12V. LDV output is filtered using input low-pass filter in order to avoid effects of excited high frequency modes on controller. Filtered output is then fed to positive input channel of op-amp via a resistor, Rc.

3.4 Experimental Setup

Experiments are conducted to investigate effectiveness of analog velocity feedback controller. Based on information given in chapter 2, it is already shown that southwest and northwest locations are effective for excitation of second and third modes of the smart plate. Minimum and maximum voltage limitation of the piezoelectric patches are -100V

and 400V. High voltage amplification for piezoelectric actuators is achieved with an amplifier,E-413.D2 Duraact Piezo Driver which is supplied by PI tech. Control input voltage between -2V and +8V are accepted by amplifier and the signal is amplified by factor of 50. The feedback signal must be between the limits of the amplifier and the patch hence, during tuning of the proportional gain, it is necessary to stay within limits. During processing of the signal, also phase lead/lag must be eliminated due to the unstability concerns. RC analog filter is designed as explained in previous sections. For RC low-pass analog filters, cut-off frequency is defined as $1/2\pi RC$. This is the frequency at which the transmitted signal decreases in magnitude 3dB. For this application, it is appropriate to choose one 330 Ohm resistor and 10μF capacitor. The cut-off frequency of the low-pass filter is 48.2 Hz. In Figure 3.3, components of the experimental set-up are shown.

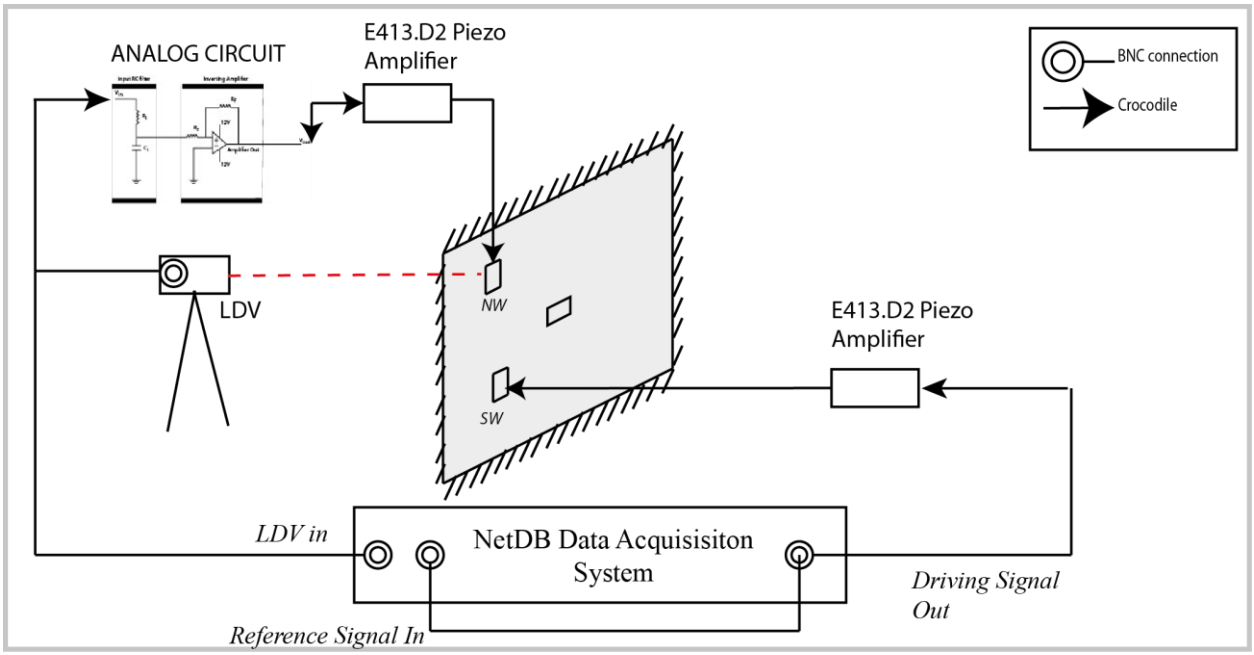

Figure 3. 3 Experimental Set-up

LDV output is fed to input low-pass filter. The filtered voltage signal is then amplified and inverted by inverting amplifier. For the inverted amplifier configuration, Rf is chosen as 10kOhm while Rc is chosen as 1kOhm to achieve a gain of 10.

Data analysis and FRF measurements are completed using NetDB data acquisition system. NetDB is a data acquisition unit with 12 analog input channels and 2 analog output channels. It communicates with a PC through ethernet connection and allows high frequency sampling with high measurement accuracy. For open loop and closed loop FRF measurements, a sine sweep signal is generated using the NetDB system. For FRF measurements, relation between the output of LDV and voltage value generated by NetDB system is also acquired.

Two different experiments are performed to show effectiveness of the controller. In the first experiment, only center patch is activated to attenuate vibrations of the smart plate. A collocated sensor and actuator pair is used in this experiment.

In the second experiment, only one patch at the northwest is activated and collocated sensor at this location this is used to create the control signal.

3.5 Results

In this section, active vibration suppression of the smart plate with analog proportional velocity feedback implementation is presented. The experimental results are given in frequency and time domains for two different piezoelectric patch configurations. The modal characteristics of the smart plate under effect of various controller gains are

investigated. Piezoelectric patches located on northwest and center of the plate are used as control actuators and southwest patch is used as the disturbance source.

3.5.1 Vibration Suppression with Center Patch

In this subsection, result of the vibration attenuation with center patch is presented. As explained in chapter 2, center patch is effective on the first mode of the plate. For that reason, controller is designed focusing on the first resonance mode of the smart plate

3.5.1.1 Frequency Response of the Controller

Effectiveness of the analog proportional velocity feedback controller is analyzed for open loop and closed loop cases. Smart plate is excited with southwest patch and the response of the plate is measured with Laser Doppler Vibrometer (LDV). Open loop frequency response of the system is obtained while controller is inactive and closed loop frequency response is obtained after the controller is activated. Frequency domain measurements are completed with the configurations described in chapter 2. Frequency domain performance of the open loop and closed loop system is presented in Figure 3.4

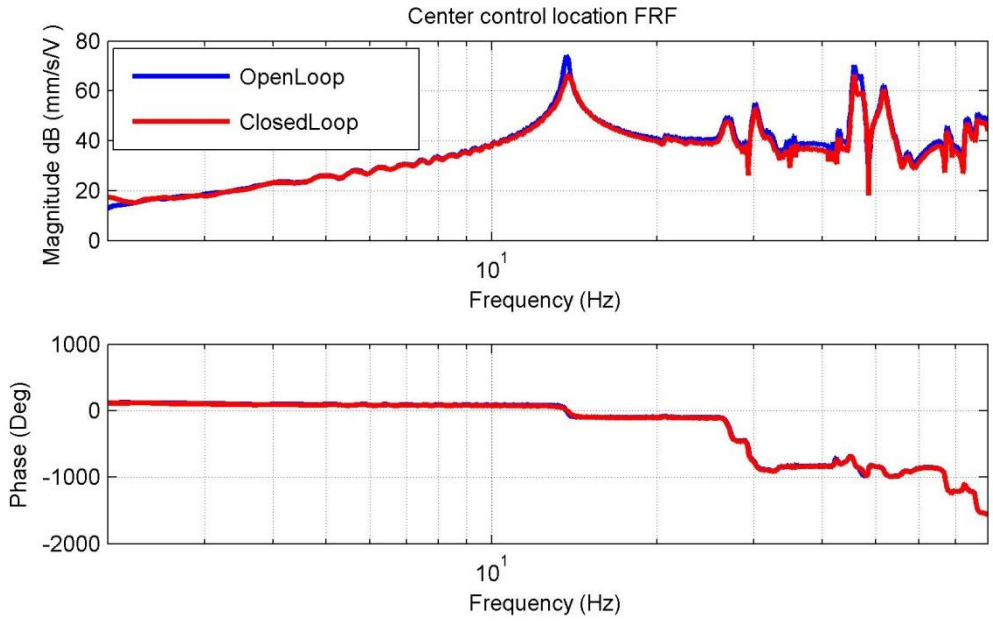

Figure 3. 4 Frequency Response of the Open Loop and Closed Loop System for Center Patch

Vibration attenuation achieved at the first mode is 7.9 dB. For second and third modes effectiveness of the controller is not significant as expected. Center of the plate is low strain region for second and third modes. For that reason, piezoelectric actuator loses its effectiveness at those regions. At the fourth mode the controller suppresses vibration around 6 dB.

3.5.1.2 Time Domain Analysis

3.5.1.2.1 First Mode Performance

In order to complete single frequency forced vibration for the first mode a sinusoidal signal with frequency of 13.67 Hz is created using NetDB system. In the beginning of the

analysis controller is inactive and at the 4th second of the experiment controller is activated. In this configuration piezoelectric patch at the center of the plate is used. Resultant response of the smart plate is measured with LDV. Response of the plate is also recorded using NetDB. In Figure3.5 time domain response of the smart plate for the first mode is presented.

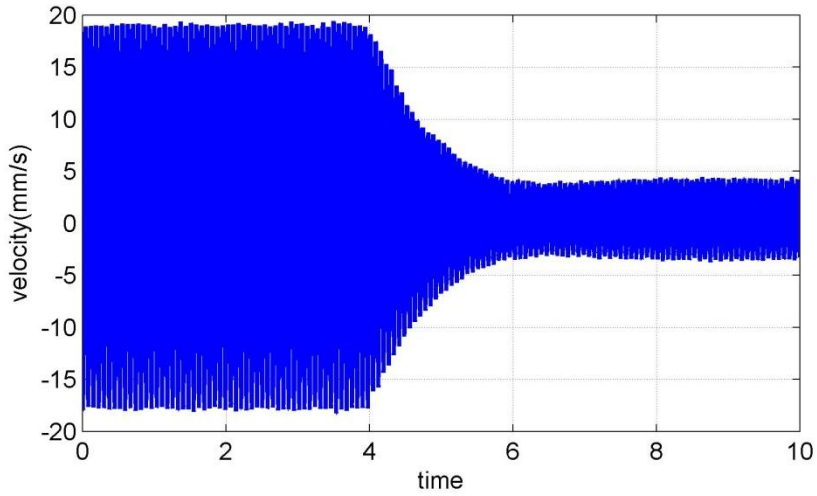

Figure 3. 5 Time Response of the Plate at the Center Location for the First Mode

Before controller is activated, response of the plate is around 36 mm/s. After activating the controller at 4th second, magnitude of the oscillation decreases to 8mm/s.

3.5.1.2.2 Fourth Mode performance

Time domain analysis is also performed for the fourth mode. In this case system is excited with frequency of 45.6 Hz where fourth mode of the smart plate is observed. In Figure3.6, the fourth mode response of the smart plate is shown when the controller is again activated at 4th second. In the open loop configuration, response of the smart plate is around 20 mm/s peak to peak but upon activation of the controller response of the smart plate decreases to 11mm/s peak to peak.

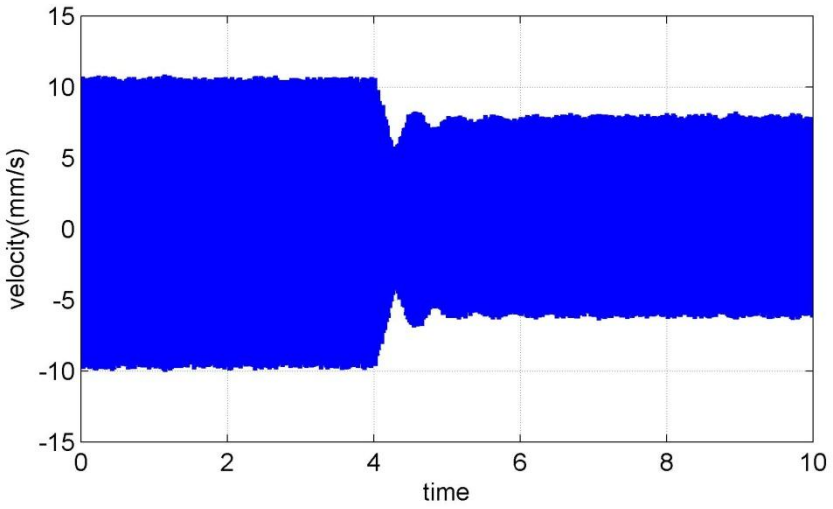

Figure 3. 6 Time Response of the Plate at the Center Location for the Fourth Mode

3.5.1.2.3 Performance of the Controller for Different Gains

In this section, effect of the different controller gains on the modal behavior of the smart plate is investigated. Three different controller gains are applied to the smart plate. Open loop and closed loop analysis of the smart plate is completed and frequency responses of the closed loop and open loop cases are compared. Configuration of the frequency domain analysis for closed loop and open loop cases are the same with the configuration given in chapter 2. In Figure3.7, the frequency responses of the smart plate in open loop and closed loop configurations are shown.

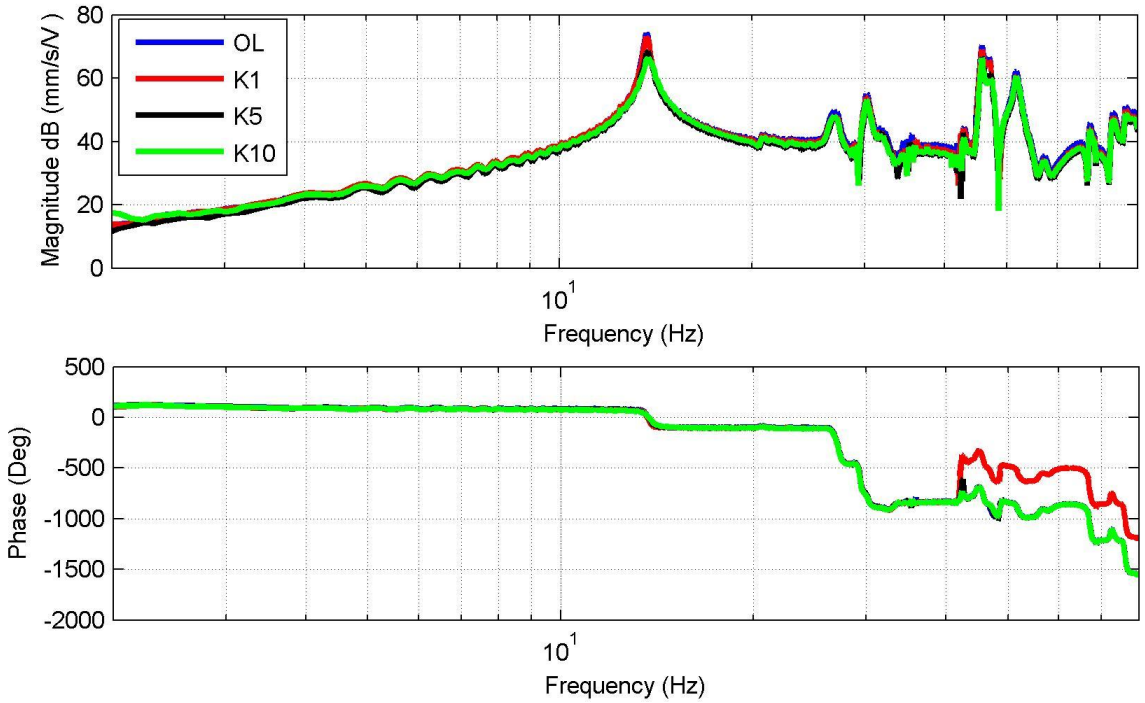

Figure 3. 7 FRF for Center of the Smart Plate under Varying Controller Gains

Controller gain is set to 1, 5 and 10.Performance of the controller increases as the gain is increases. But slight shifts on resonance frequencies are observed. In Figures 3.8 and 3.9, the magnitude and frequency changes are shown. Frequency shift is not observable for the second and fourth modes when the center patch is used as actuator. At the first mode of the plate, increasing gain leads to increasing modal frequency shifts. But for the third mode, the lowest applied gain increases the frequency of the vibration mode. In general, an increase on the modal frequencies of the smart plate is observed as the controller gain is increased.

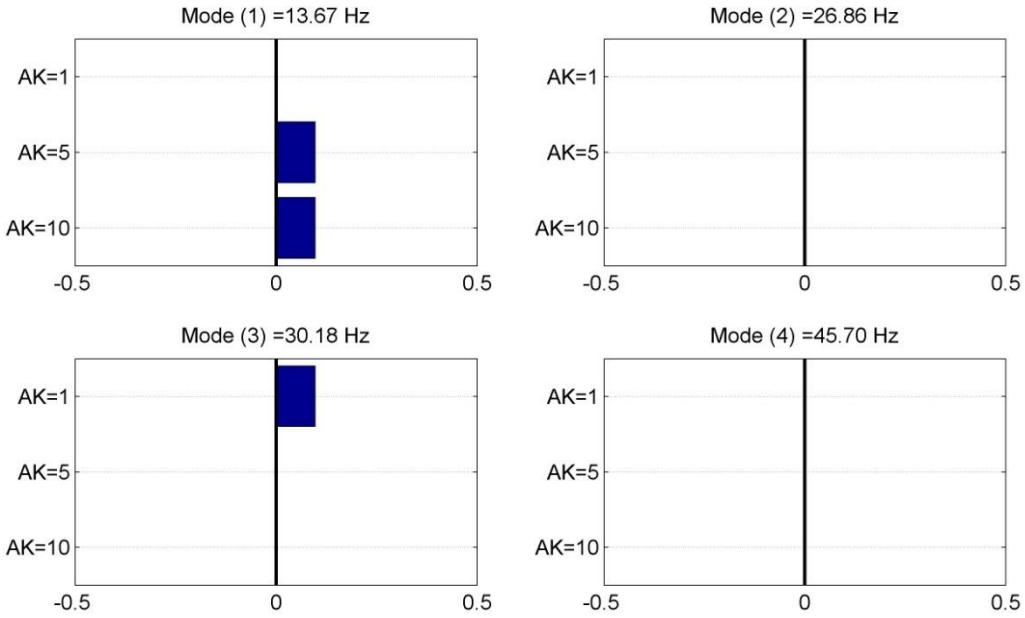

Figure 3. 8 Change in Modal Frequencies for Different Controller Gain.

In Figure3.9, magnitude responses of the controller are given for varying gain. According to the analysis for 1st and 4th modes increasing gain leads to higher performance of the controller. In the second and third modes, best performance is achieved when the controller gain is equal to 5. But the performance for second and third modes are negligible since center of the plate is not effective in the second and third modes.

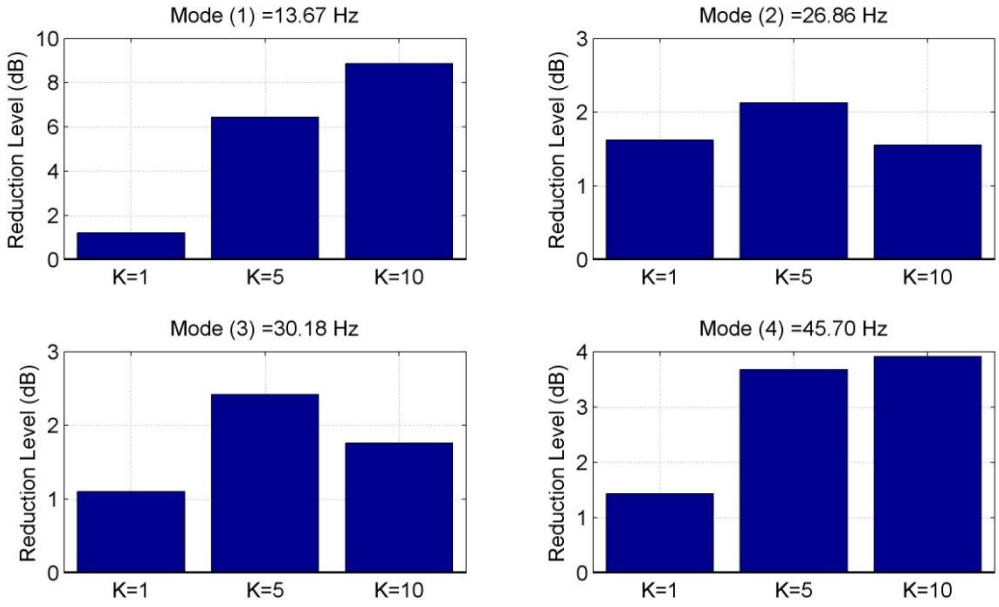

Figure 3. 9 Change in Magnitudes of Frequency Responses for Different Controller Gains

3.5.2 Vibration Suppression with Northwest Patch

In this subsection, result of the vibration attenuation with northwest patch is presented. Controller gain is adjusted to get the best performance in the first mode. For further analysis of the controller, different gains are applied and changes in vibration characteristics of the smart plate is investigated.

3.5.2.1 Frequency Response of the Controller

Frequency response analysis of the controller designed for northwest patch is completed for open loop and closed loop cases. Southwest patch is used to excite the smart

plate and Laser Doppler Vibrometer is used to measure the response. For open loop analysis, controller is deactivated and the measurements are completed. In closed loop analysis, measurements are completed after controller is activated. Frequency domain performance of the open loop and closed loop behavior of the controller is presented in Figure3.10.

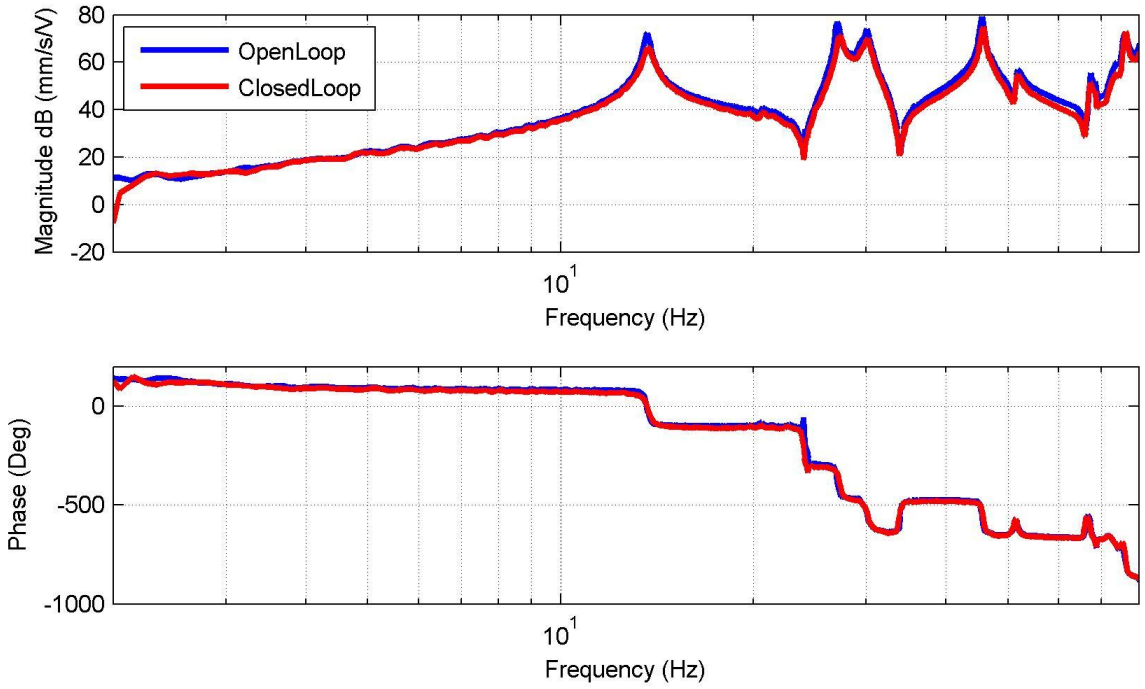

Figure 3. 10 Frequency Response of the Open Loop and Closed Loop System for Northwest Patch

In the first mode of the smart plate controller suppresses vibration around 6.5 dB. In this case, second and third modes are also obvious. Controller performance for the second third and fourth modes are 6dB, 5dB, and 6dB, respectively.

3.5.2.2 Time Domain Analysis

3.5.2.2.1 First Mode Performance

In order to complete time domain measurements for the first mode a sinusoidal signal with frequency of 13.67 Hz is created using NetDB system. In the beginning of the analysis controller is inactive and at the 4th second of the experiment controller is activated. Resultant response of the smart plate is measured with LDV. Response of the plate is also recorded using NetDB system. In Figure3.11, time domain response of the smart plate for the first mode is presented.

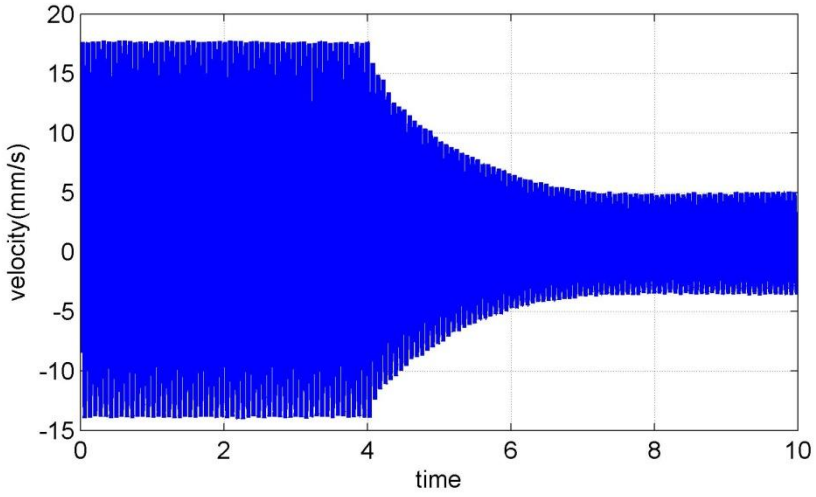

Figure 3. 11 Time Response of the Plate at the Northwest Location for the First Mode

Open loop behavior of the smart plate indicates that, without control, response of the plate is around 30 mm/s peak to peak. After activating the controller at 4th second, magnitude of the oscillation decreases to 9 mm/s peak to peak.

3.5.2.2.2 Second Mode Performance

Same procedure for time domain analysis for the second mode is followed. Here, frequency of the sinusoidal signal is adjusted to 27.03 Hz where second mode of the system is observed In Figure3.12 second mode response of the smart plate is time domain is shown.

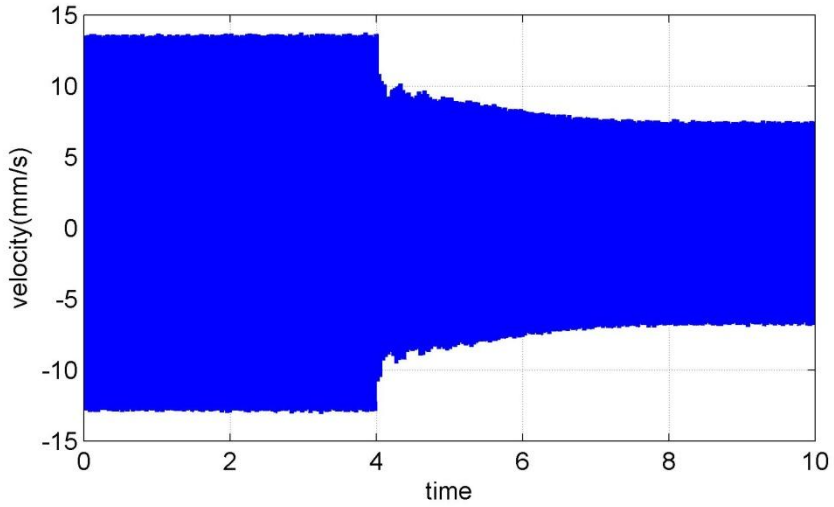

Figure 3. 12 Time Response of the Plate at the Northwest Location for the Second Mode

Open loop response of the plate is around 24 mm/s peak to peak. After activating the controller at 4th second, magnitude of the oscillation decreases to 13 mm/s peak to peak

3.5.2.2.3 Third Mode Performance

Analysis of the smart plate for the third mode in time domain is also performed. For this purpose, system is excited with a sinusoidal signal at the frequency of 30.3 Hz where

third resonance of smart plate is observed. Time domain behavior of the smart plate in third mode is indicated in Figure 3.13

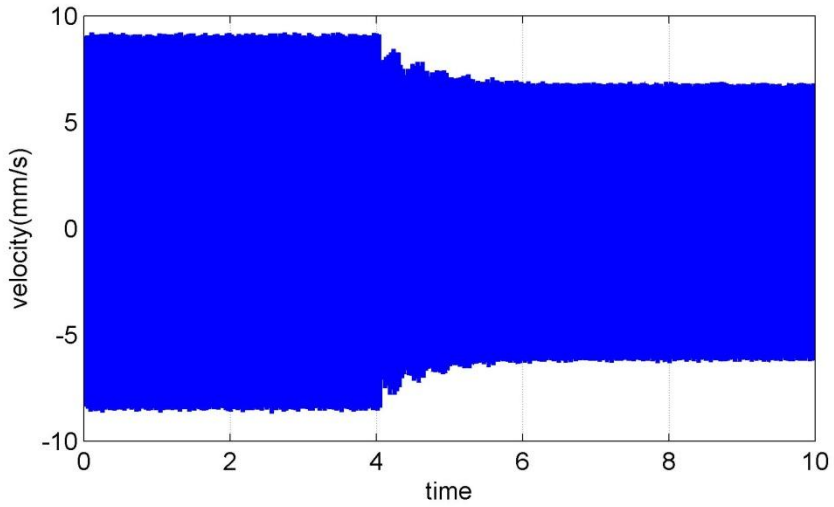

Figure 3. 13 Time Response of the Plate at the Northwest Location for the Third Mode

Magnitude of the response in open loop case is 16 mm/s peak to peak. Activation of the controller at 4^{th} second, leads to decrease in magnitude of the oscillation to 12 mm/s peak to peak.

3.5.2.2.4 Fourth Mode Performance

Time domain behavior of the smart plate is also observed for the fourth mode. For this purpose, a sinusoidal signal at 45.6 Hz is created to excite the smart plate. In Figure

3.14, time domain behavior of the smart plate for the fourth mode is shown. Before the controller is activated, response of the plate is around 38 mm/s peak to peak. After activating the controller at 4th second, magnitude of the oscillation decreases to 15 mm/s peak to peak.

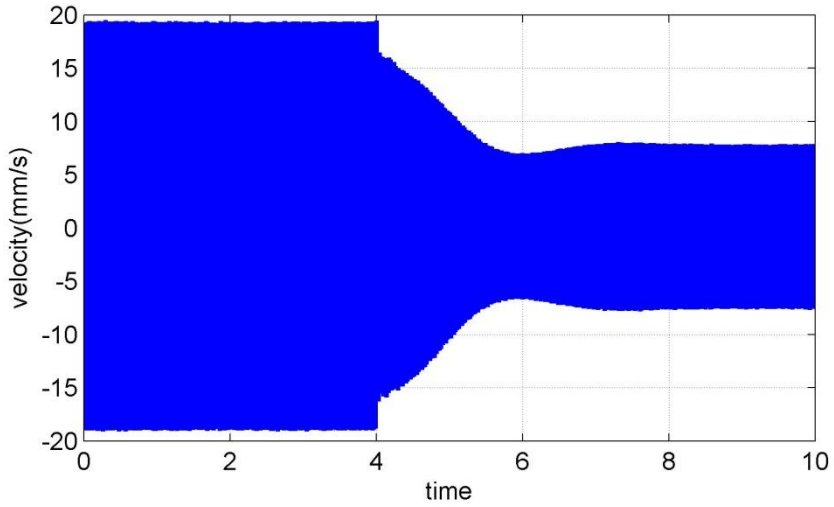

Figure 3. 14 Time Response of the Plate at the Northwest Location for the Fourth Mode

3.5.2.3 Vibration Characteristics Analysis of Different Gains

In this section effect of the different controller gains on the modal behavior of the smart plate is investigated. Three different controller gains are applied to the smart plate. Open loop and closed loop analysis of the smart plate is completed in each configuration and results of those cases are compared. Experimental set up for the frequency domain analysis in closed loop and open loop cases are the same with the configuration explained

in chapter 2. In Figure3.15 frequency responses of the smart plate in open loop and closed loop cases are shown.

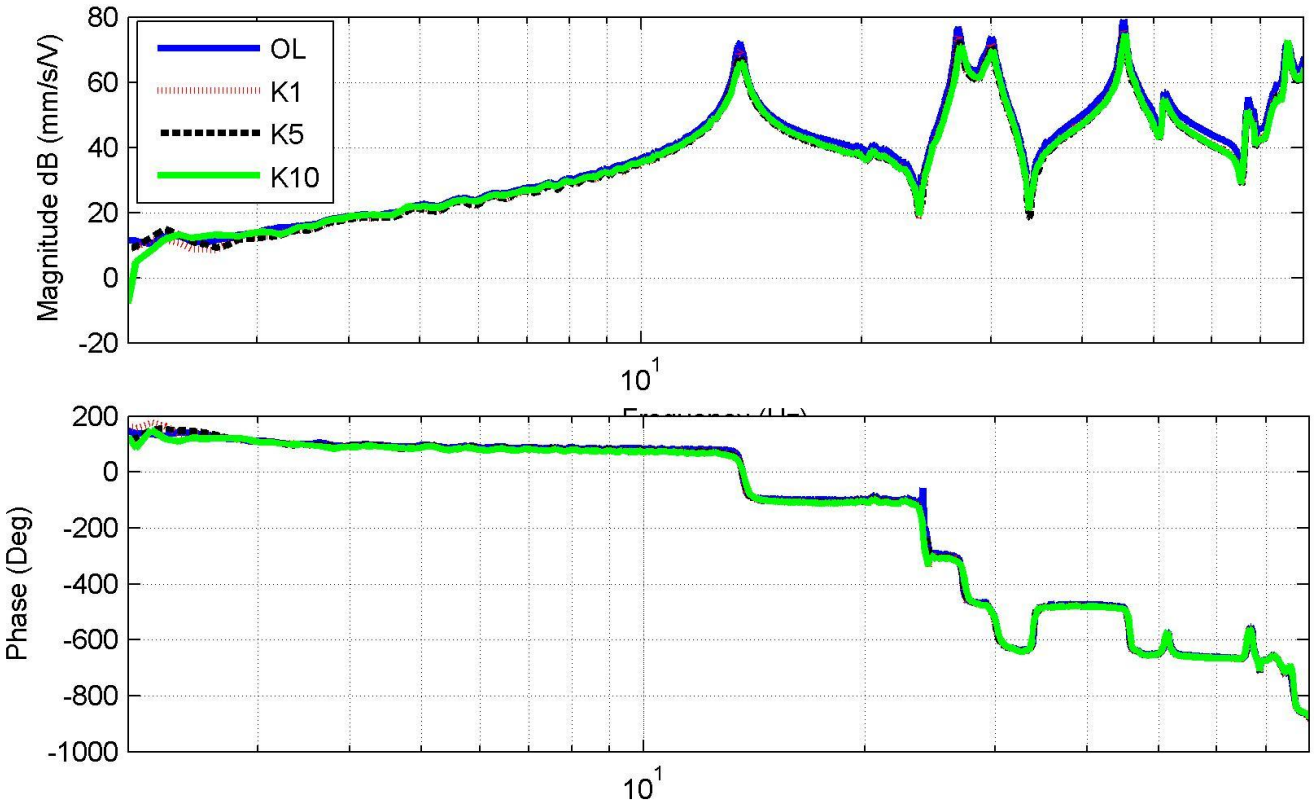

Figure 3. 15 FRF for Northwest of the Smart Plate under Varying Controller Gains

Controller gain is set to 1, 5 and 10 respectively. Increase in the performance of the controller for increasing gain is observed..In resonance frequencies slight shifts are observed. In Figures3.16 and 3.17 magnitude and frequency changes of the resonances of smart plate under closed loop cases are shown. Results indicate that at the first mode, modal frequency remains unaltered. In the second and third modes, when the gain is

adjusted to 1, modal frequency remains unaltered but as the gain is increased, modal frequency tends to increase. For the fourth mode, modal frequency tends to increase even when the gain is set to 1. It is also obvious that for the first four modes, increasing gain creates tendency to increase modal frequency.

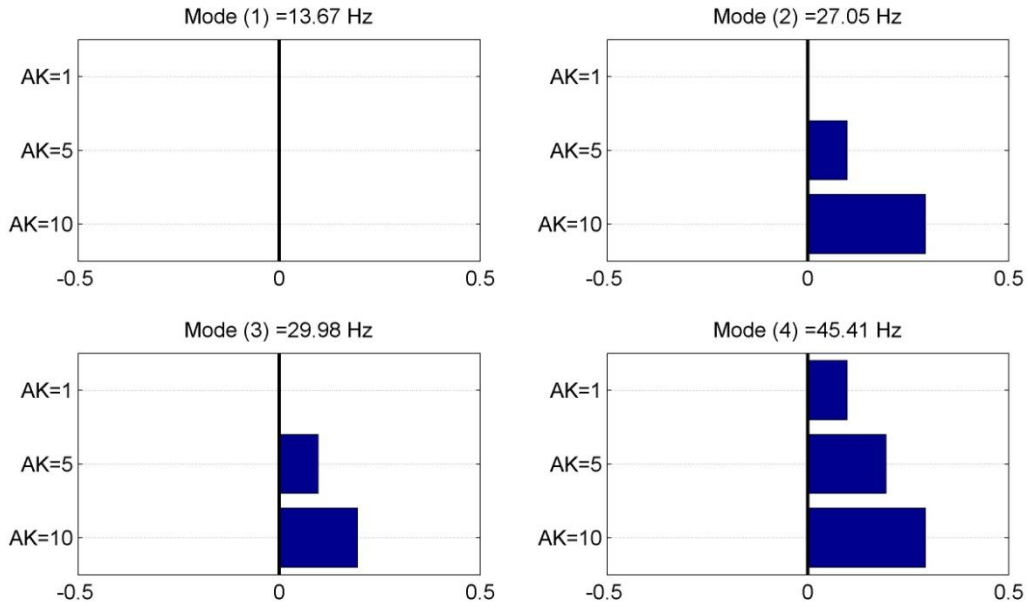

Figure 3. 16 Change in Modal Frequencies for Different Controller Gains

Besides analysis in modal frequencies, effect of the controller on the magnitude of the frequency response is also investigated. In Figure3.17 change in magnitude of the frequency response is plotted for first four modes. In each mode the effect of the varying gain is also shown.

Increasing gain of the controller creates tendency to decrease the magnitude of the response of smart plate. The best suppression is available when gain is equal to 10.

Although all controller gains are effective in vibration suppression, it is obvious that increasing gain up to ten yields better performance for first four modes.

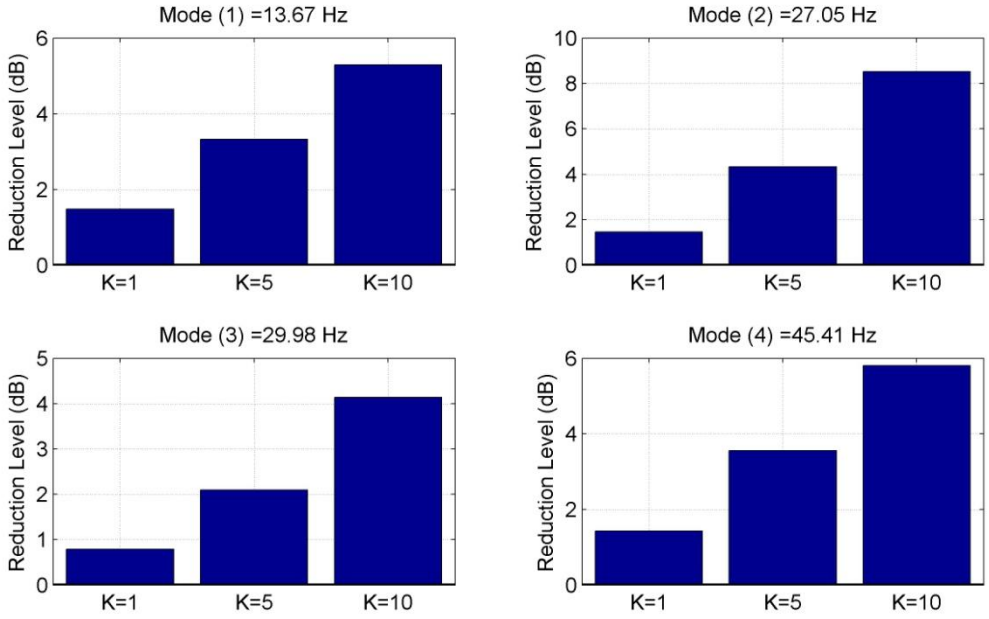

Figure 3. 17 Change in Magnitudes of Frequency Responses for Different Controller Gains

3.6 Conclusion

In this chapter, effectiveness of the analog proportional velocity feedback controller is analyzed. Besides controller effectiveness, modal behavior of the smart plate is investigated when the controller included is activated.

Controller performance analysis is conducted for two different piezoelectric actuators those are located at center of the plate and northwest of the plate. In both cases, LDV is used as disturbance sensors and control actuators are center patch and northwest patch respectively. For control system design collocated sensor-actuator pair structure is chosen for stability. An analog circuit is built as proportional velocity feedback controller and controller gain is adjusted manually until best performance control performance is achieved for the first mode in both cases. Result for center patch showed that, center patch is not effective for second and third modes of the plate. For second and third modes center of the smart plate is low strain region. Piezoelectric patches create strain to operate so center patch lacks effectiveness for second and third modes. But northwest patch performs for second and third modes as well.

Effectiveness of the controller on the modal behavior of the smart plate is analyzed with the same configuration. In those experiments, for different controller gains, how smart plate performs under control is analyzed. For center patch frequency shift is obscure but for northwest patch frequency shift is clear. Results showed that increasing gain creates tendency to increase resonance frequency.

CHAPTER 4

STUDY ON SUPRESSING VIBRATION OF THE SMART PLATE WITH DIGITAL CONTROL SYSTEMS

4.1 Introduction

In this section, vibration suppression of the smart plate with a digital controller implementation is presented. For this purpose, two feedback algorithms are designed and implemented. Performances of implemented algorithms are compared and changes in vibration characteristics of the smart plate due to the controller implementation are analyzed.

In the first half of this chapter, experimental analysis of the digital proportional velocity feedback controller is performed on the smart plate. Frequency domain and time domain analysis of the performance of the open and closed loop system are used as an evaluation criteria for the effectiveness of the controller.

In the second half of this chapter, optimal state feedback controller is designed and implemented. Controller performance is analyzed in frequency and time domain. Analysis on the smart plate is performed for open loop and closed loop cases. Modal behavior of the smart plate is also investigated to see the resonance frequency shifts when the controller is implemented.

4.2 Digital Controller

In this section, design and implementation procedure of the digital feedback controllers is presented. Controller theory with design objective and experimental set up for controller performance evaluation are introduced.

4.2.1 Proportional Velocity Feedback Controller

In theory, analog and digital implementation of the proportional velocity feedback controller is not different. Refer to chapter 3 for further details.

4.2.1.1 Control System Design

In this section design of proportional velocity feedback controller is presented. Design procedure of the controller is very similar to the analog controller design which was explained in the previous chapter. Here again, phase lead/lag is the main problem for the stability of the controller. Excitation of the higher frequencies would detoriate the stability and such problem can be avoided either by decreasing the controller gain or including a low pass filter in the system.

Low pass filters reduce amplitudes of the signals with frequencies higher than the cut-off frequency. Here, cut-off frequency stands for the frequency at which low-pass filter decreases magnitude by 3dB. In continuous time, low pass filters are represented by the transfer function given in eq 4.1

$$G(s) = \frac{\omega}{s+\omega} \qquad 4.1$$

Where ω stands for $2\pi f_{cut-off}$. Since the controller operates in discreete time, upon definition of the transfer function of the low-pass filter in continous time, it is necessary to convert the continous time filter transfer function to discreete time. For this purpose, c2d

function in MATLAB's control toolbox is used. It is designed for conversion between continuous time linear time invariant (LTI) system representations to discrete time LTI representations. The function accepts the continuous time model and sampling frequency of the digital application and conversion method in order to convert the model. In this study zero-order hold method is used for conversion. For the conversions, sampling frequency is adjusted as 70000 Hz at which digital controller operates.

Upon processing for discrete time the formation of the filter transfer function becomes

$$G_{filter}(z) = \frac{a}{z + b} \tag{4.2}$$

Here a and b are design parameters for the low pass filter and their sum must be equal to 1. In this study, cut-off frequency of the low-pass filter is 50 Hz and values of a and b are equal to 0.9955 and 0.0045 respectively.

Controller gain is adjusted with trial error method. Starting from gain 1, gain is increased step by step and the gain for achieving best performance for the first mode is determined as the tuned gain used for the proportional velocity feedback controller.

4.2.2 Optimal State Feedback Controller

In this section, design and implementation of the optimal state feedback controller is presented. For this purpose, system identification of the plant dynamics and the procedures for controller implementation are explained in detail.

4.2.2.1 Optimal Control Law

In the first step, it would be convenient to explain what optimal control is. Optimal control of a system would be defined using the representation below:

$$u^*(t) = f(x(t), t) \tag{4.3}$$

Functional,*f*, shown in equation 4.3 is called optimal control law or optimal control policy. Aim of such a definition is that to generate an optimum feedback using current measures of state at a given time. The presence of time, *t*, in optimal control law indicates that the optimal control feedback gain is dependent on time.

Optimality of a decision making for a controller would be defined as follows. Think of a starting point a and aim to reach a point c through an intermediate point b. Optimality requires a path following the shortest possible combination of connection for those points. [45]

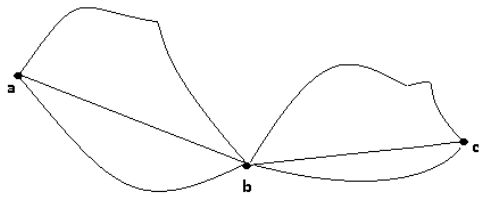

Figure 4. 1 Optimality Problem, Path Selection

In Figure 4.1[45] there are 9 different alternatives to reach point c from point a through point b. Aim of the optimal theory is to choose the shortest possible way to reach the desired state starting from an initial state. The way between the initial and final states is optimized using cost functions. Cost functions have two different components. Those are the ones related to current value of the state and ones related to current control input. Since those two change dynamics of the system, it is necessary to think of the effects of those for

an optimization problem. A cost function defined as follow is the most basic form of optimal control cost function

$$J = x^2(T) + \lambda \int_0^T u^2(t) \qquad (4.4)$$

Where *T* is the final time and *J* allows adjustment of two terms through , which is called weighting. *x(T)* and *u(t)* are squared since negative or positive terms of those values have equal importance. Such a performance measure indicated in *J* reflects desire to drive final state close to its desired value without excessive expenditure of control effort. Amount of effort for control system is regulated by the weighting included in cost function.

4.2.2.2 Linear Quadratic Regulators

Linear quadratic regulator aims to minimize integral square error by minimizing cost function *J* over a time interval. In linear regulation problem the optimal control law can be determined in the form of a linear time-varying function which, under certain conditions" can become time invariant.

The plant interested in this optimality problem is described by linear state equations and given by:

$$\dot{x}(t) = A(t)x(t) + B(t)u(t) \qquad (4.5)$$

The aim of the control law is to minimize the cost function J which is the performance measure and given by:

$$J = \frac{1}{2}X^t(t_f)Hx(t_f) + \frac{1}{2}\int_{t_0}^{t_f}[X^T(t)Q(t)X(t) + U^T R(t)U(t)]dt \tag{4.6}$$

Here X is state vector and U is input vector. Q and R are called weighting matrices. For a particular linear quadratic regulator design, tuning parameters are those two matrices.

The final time is fixed ("t_f"), H and Q are real symmetric positive semi-definite matrices, and R is a real symmetric positive definite matrix. It is assumed that the states and controls are not bounded, and $x(t_f)$ is free. It is desired to maintain the state vector close to the origin without an excessive expenditure of control effort.

In order to obtain a solution to such problem, matrix Riccati equations are used. Following equation is the general form of the Riccati equations for optimum solution in LQR.

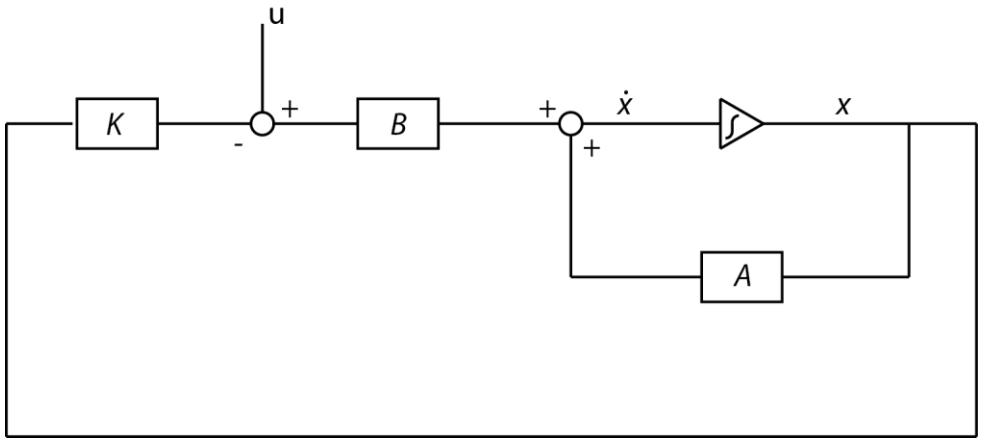

Figure 4. 2 Block Diagram for LQR

$$\dot{K}(t) = -K(t)A(t) - A^T(t)K(t) - Q(t) + K(t)B(t)R^{-1}(t)B^T(t)K(t) \tag{4.7}$$

With the boundary condition $(t_f) = H$. Here H stands for the Hamiltonian. For further information for the steps of the solution please refer to [45].

These equation can be integrated numerically by a digital computer by starting the integrating at $t = t_f$ and proceeds backwards in time to $t = t_0$ $K(t)$ is stored and solution of the cost function leads to an optimal gain matrix, K, which is used in calculating optimal input such that :

$$u(t) = -Kx(t) \tag{4.8}$$

Where x is state vector. For a time interval specified by, cost function is solved using iterative methods but as the final time goes to infinity, optimal gain matrix K, is the riccati solution of the cost function. In Figure4.2, block diagram for the Linear Quadratic Regulator is shown.

4.2.2.1 System Identification and Modeling

In this section, the procedure for the system identification of the smart plate is presented. In all cases, frequency domain behavior of the smart plate is measured and frequency response functions are extracted. For further analysis, MATLAB is used for modeling and control system design.

FRF measurements of the system are performed using piezoelectric actuator, LDV and NetDB data acquisition system. Piezoelectric actuators are bonded on the surface. A sine sweep signal is created to drive piezoelectric patch with output channel of the NetDB system and this signal is specified as the reference signal for the FRF measurement. LDV is

used to acquire data on the sensor location and this information is transmitted to the NetDB system.

NetDB system completed frequency domain data acquisition and the results are saved for further processing. During the measurements, piezoelectric patch is driven with the sinesweep signal. It took 50 seconds for the signal to increase from 0 Hz to 100 Hz. Vibration data is collected with block size of 4096. 57 averages are taken to generate better results. Frequency span chosen is up to 156 Hz. In Figure4.3 experimental set-up for FRF acquisition is shown.

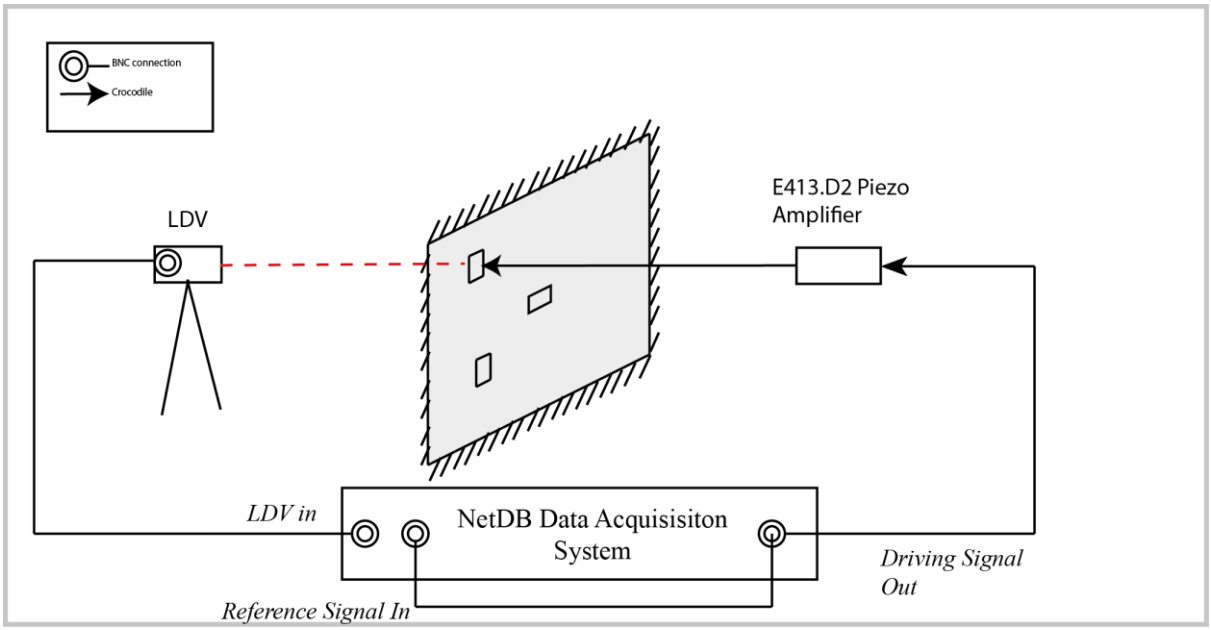

Figure 4. 3 Experimental Set-Up for System Identification

Model of the smart plate is created based on the FRF measurements. A state space model is fitted to the FRF using MATLAB. In model based controllers, state space model

is the method for system representation. For dynamic system, the state of a system is described in terms of a set of state variable

$$x = [x_1(t)\ x_2(t)\ x_3(t)\ \dots\ x_n(t)] \tag{4.9}$$

State variables describe the present configuration of the system and can be used to determine the future response given the excitation inputs and the equations describing the dynamics[46].

Response of a system is described as set of first order differential equations written in terms of state variables and the inputs. These first order differential equations can be written as

$$\begin{aligned}
\dot{x}_1 &= a_{11}x_1 + a_{12}x_2 + \dots + a_{1n}x_n + b_{11}u_1 + \dots + b_{1m}u_m \\
\dot{x}_2 &= a_{12}x_1 + a_{22}x_2 + \dots + a_{2n}x_n + b_{21}u_1 + \dots + b_{2m}u_m \\
&\vdots \\
\dot{x}_n &= a_{n1}x_1 + a_{n2}x_2 + \dots + a_{nn}x_n + b_{n1}u_1 + \dots + b_{nm}u_m
\end{aligned} \tag{4.10}$$

In this representation $\dot{x} = \frac{dx}{dt}$ and those set of equations can be converted to matrix formation as in eq 4.11

$$\frac{d}{dt}\begin{bmatrix} x_1 \\ x_2 \\ \cdot \\ \cdot \\ x_n \end{bmatrix} = \begin{bmatrix} a_{11} & a_{12} & \dots & a_{1n} \\ a_{21} & a_{22} & \dots & a_{2n} \\ \vdots & \vdots & \ddots & \vdots \\ a_{n1} & a_{n2} & \dots & a_{nn} \end{bmatrix} + \begin{bmatrix} b_{11} & \dots & b_{1m} \\ \vdots & \ddots & \vdots \\ b_{n1} & \dots & b_{nm} \end{bmatrix} \begin{bmatrix} u_1 \\ \vdots \\ u_m \end{bmatrix} \tag{4.11}$$

The column matrix consisting the state variables is called the state vector and written as

$$X = \begin{bmatrix} x_1 \\ x_2 \\ \cdot \\ \cdot \\ \cdot \\ x_n \end{bmatrix} \tag{4.12}$$

The vector of the input signal is defined as u. Then the system can be represented by the compact notation of the state differential equations

$$\dot{x} = Ax + Bu \tag{4.13}$$

A is the square matrix with dimension of n-by-n and B is called input matrix with a dimension of n-by-m. The state differential equation relates the rate of change of the state vector to the state of the system and the input given to the system. The outputs of the system are related to the state variables and the input signals by the output equation

$$y = Cx + Du \tag{4.14}$$

Where y is the set of output signals, expressed in column vector form. The state space representation comprises the state differential equation and the output equation[46].

In this study, state representation of the plant is created using fitsys command of MATLAB and the states do not have any physical meaning.

The matrices A,B,C and D are also created by the least square algorithm utilized by fitsys and they have no specific physical meaning either.

Based on the experimental evaluation of the smart plate, a state space model is fitted to measurements completed in frequency domain. Experimental analysis of the frequency domain behavior of smart plate is completed with NetDB system and for further analysis, frequency domain data is transferred to MATLAB.

fitsys command of the mu analysis toolbox of MATLAB, is used for processing of data and creation of the model for smart plate. Least squares method is preferred modelling algorithm for fitsys. Actual experimental data, the range of frequency for modelling, order of the state space model must be selected for fitsys command to process the system identification. Besides those parameters, the stability condition is optionally adjusted by the user. The actuator model required for the state feedback control In this case, the control actuator is the northwest piezoelectric patch. System identification procedure is applied for the northwest piezoelectric patch using the frequency response.(See figure 4.4)

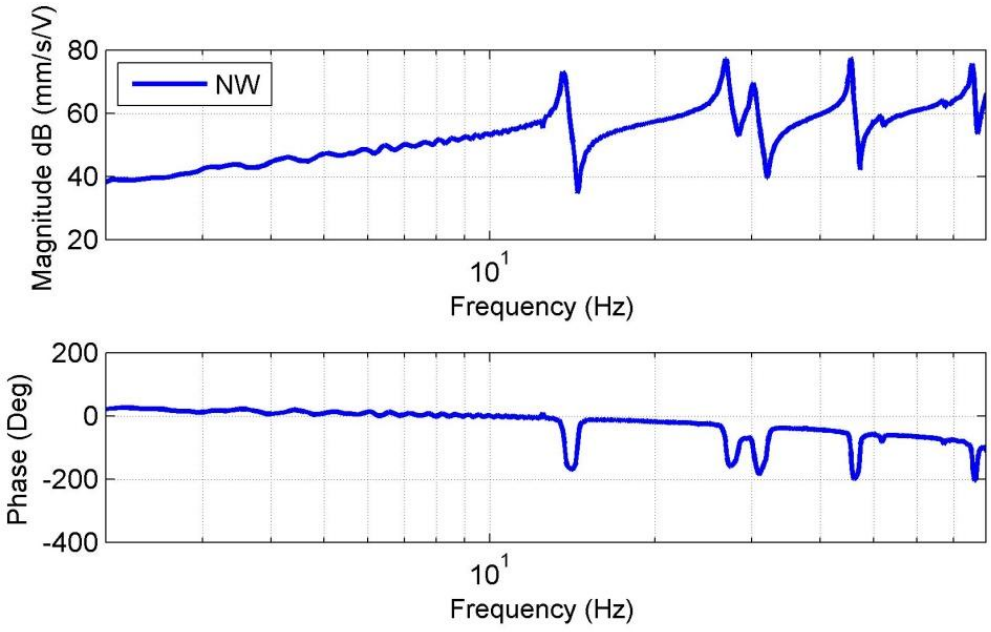

Figure 4. 4 FRF for Northwest Patch

For the control application, aim is to suppress first four modes of the smart plate. Thus, it is necessary to create a model including dynamics of the first four modes. Using "fitsys" function of the MATLAB, a state space model is created. State space model is created as continuous time model. Using "c2d" command of MATLAB, the model is converted to discrete time. A 10th order model is found to be sufficient to represent dynamics of the first four modes. In equation 4.15 A,B,C and D matrices of the state space model are shown

$$A=\begin{bmatrix} 1 & -0.004 & 0 & 0.0001 & 0 & 0 & 0 & 0 & -0.0002 & -0.0001 \\ 0.004 & 1 & -0.0005 & 0 & 0 & 0 & 0 & 0 & -0.0001 & 0 \\ 0 & 0.0005 & 1 & 0.0024 & 0 & 0 & 0 & 0 & -0.0002 & 0 \\ -0.0001 & 0 & -0.0024 & 1 & 0 & 0 & 0 & 0 & 0 & 0 \\ 0 & 0 & 0 & 0 & 1 & -0.0012 & 0 & 0 & -0.0001 & 0 \\ 0 & 0 & 0 & 0 & 0.0012 & 1 & 0 & 0 & 0 & 0 \\ 0 & 0 & 0 & 0 & 0 & 0 & 1 & -0.0027 & -0.0002 & -0.0001 \\ 0 & 0 & 0 & 0 & 0 & 0 & 0.0027 & 1 & -0.0001 & 0 \\ 0.0002 & -0.0001 & 0.0002 & 0 & 0.0001 & 0 & 0.0002 & -0.0001 & 0.9982 & -0.0015 \\ -0.0001 & 0 & 0 & 0 & 0 & 0 & -0.0001 & 0 & 0.0015 & 0.9982 \end{bmatrix} \quad B=1e-4\begin{bmatrix} 0.1155 \\ -0.0546 \\ 0.0895 \\ 0.0134 \\ 0.0483 \\ -0.0013 \\ 0.0411 \\ -0.0331 \\ -0.3062 \\ 0.1123 \end{bmatrix}$$

$$C=[0.8073 \quad 0.3837 \quad 0.6266 \quad -0.0949 \quad 0.3380 \quad 0.0096 \quad 0.2873 \quad 0.2323 \quad 2.1452 \quad 0.7885] \qquad D=0 \qquad (4.15)$$

In Figure 4.5 fitted model is shown. From the figure it can be observed that the plant model is accurate enough to represent vibration characteristics of the first four modes.

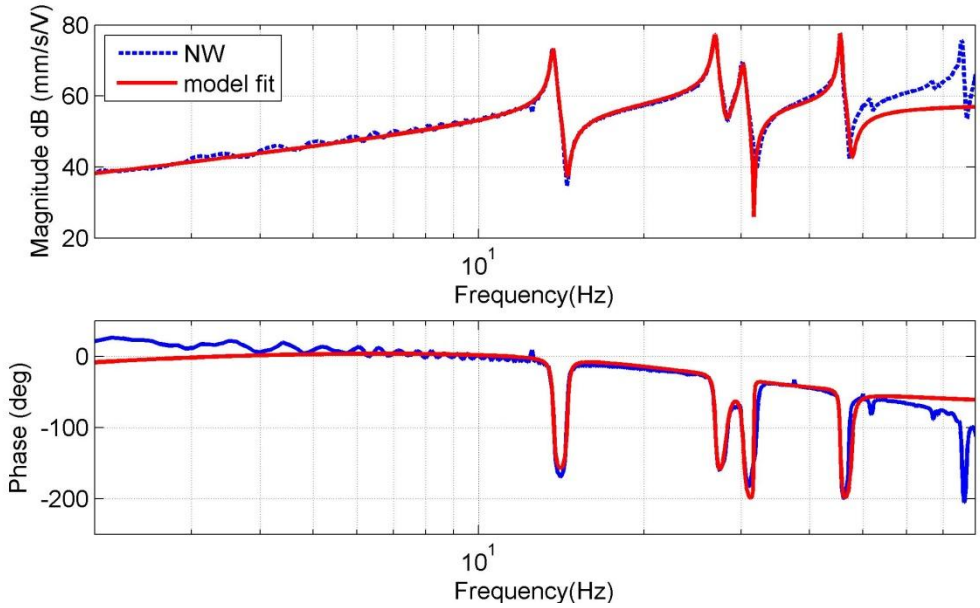

Figure 4. 5 Model Fitted to Original Response of the System.

4.2.2.3 Luenberger Observer

In this section description of Luenberger observer is given. In this thesis, since states are not directly available for measurement, it is necessary to estimate the states. An estimator is defined as constructing estimate states, $\tilde{x}(k)$ of the original states $x(k)$ by measuring the output $y(k)$ and input $u(k)$ where k indicates the current time step[47]. Luenberger observer is type of estimator that corrects the estimation equation with a feedback form of the estimation error, $y(k) - \tilde{y}(k)$ [47].

Block diagram for Luenberger observer is shown in Figure4.6[47]. It is possible to see from block diagram that the input information and output information are manipulated with current matrices of the state space representation. Estimator aims to minimize the state feedback error between actual states and observed states.

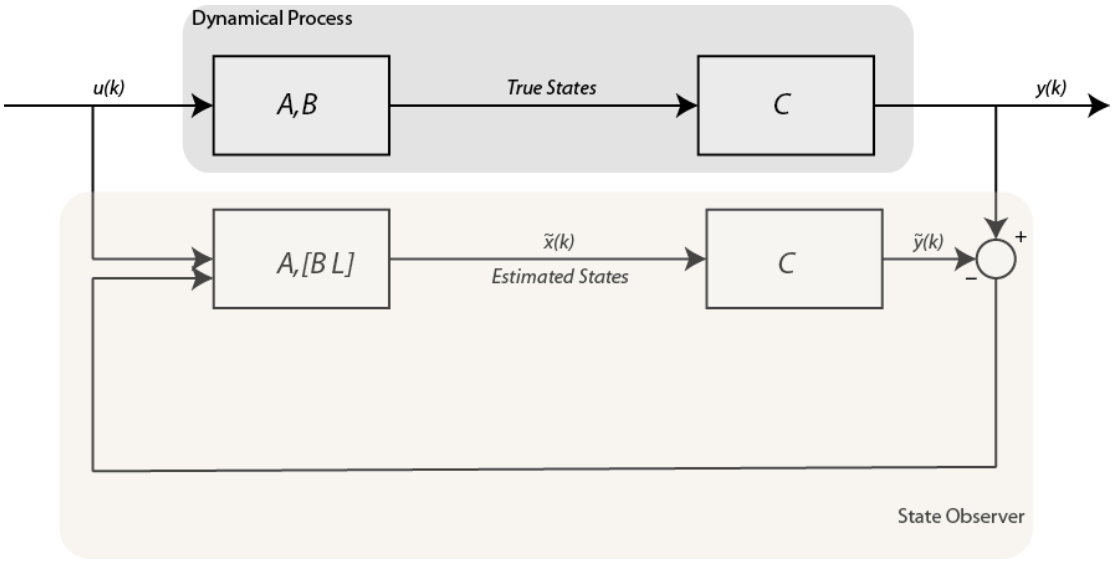

Figure 4. 6 Luenberger Observer Block Diagram

General form of the Luenberger observer is given in equation 4.16

$$\tilde{x}(k+1) = A\tilde{x}(k) + Bu(k) + \underbrace{L(y(k) - C\tilde{x}(k))}_{feedback\ on\ estimation\ error} \tag{4.16}$$

In equation 4.16 L is the observer gain matrix. Let define estimation error as $\hat{x}(k) = x(k) - \tilde{x}(k)$. Utilizing equation 4.16 and the estimation error definition the estimation error at the time step k+1 becomes

$$\hat{x}(k+1) = Ax(k) + Bu(k) - A\tilde{x}(k) - Bu(k) - L[y(k) - C\tilde{x}(k)] \tag{4.17}$$

$$\hat{x}(k+1) = (A - LC)\hat{x}(k) \tag{4.18}$$

Definition of the $\hat{x}(k)$ in equation 4.18 is as follows

$$\hat{x}(k) = (A - LC)^k(x(0) - \tilde{x}(0)) \tag{4.19}$$

Here L is the observer gain matrix and the calculation of the L is as follows. In MATLAB command 'lqr' of the control toolbox, system matrix A and output matrix C are used with their respective weight matrix as in the case of calculation for the LQR gain matrix.

4.3 Experimental Procedure

In this part, experimental set up of the digital velocity feedback controller and state feedback controller is presented. Controller is applied to the smart plate to suppress vibration of the plate. Experiments are conducted for open loop and closed loop cases.

In open loop case, southwest patch is activated as undesired vibration source. Resultant disturbance on the smart plate is measured at the northwest location of the plate with LDV. Piezoelectric patches are Dura-act P876.A12. Detailed information on the piezoelectric patches and LDV can be found in previous chapters. Signal acquired from LDV is transferred to NetDB system. Driving signal for the southwest patch is a sine-sweep signal created using output channel of the NetDB system. For proper excitation of the piezoelectric patches, piezoelectric patch amplifier is used between output channel of the NetDB system and piezoelectric patches. The driving signal fed to southwest patch is also adjusted as the reference signal for frequency domain analysis. In Table4-1 properties of the driving signal and frequency domain characteristics of the analysis is tabulated.

Table 4- 1 Properties of Excitation Signal

Signal Type	Sine Sweep
Frequency Component	2-100 Hz
Time for one cycle of signal	50 seconds
Sampling rate	51200 Hz
Block Size	4096
Frequency span	156 Hz
Duration of analysis	300 seconds
Average	57
Window type	Hanning
Overlap	%50

For closed loop frequency domain analysis, signal characteristics of driving signal and frequency domain analysis procedure remained the same. In this case, controller is activated. Northwest patch is adjusted as control actuator. Control signal is created by NI-PCI-6229 Data Acquisition unit is shown in Figure 4.7. For detailed information on specifications of the NI-PCI 6229 please refer to [48].

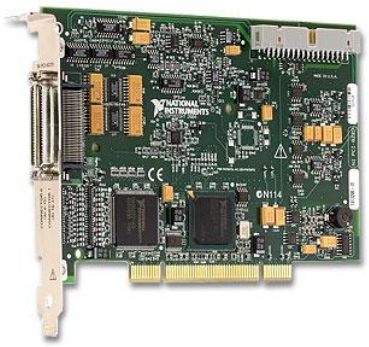

Figure 4. 7 NI-PCI 6229 DAQ Unit

LDV signal is transferred to analog input channel of the NI-PCI-6229 and control signal is created by amplifying the sensor signal. Resultant control signal is transferred to northwest patch for control actuation.

4.4 Results

In this section, results on comparison of the digital velocity feedback controller and state feedback controller are presented. For performance analysis of the controllers, frequency domain and time domain behavior of the smart plate are evaluated.

4.4.1. Frequency Response of the Controller

Performance evaluation of the digital feedback controllers is presented in this section. closed loop cases are included in both controller types. Figure 4.8 shows the performance of the proportional velocity feedback controller and the optimal state feedback controller

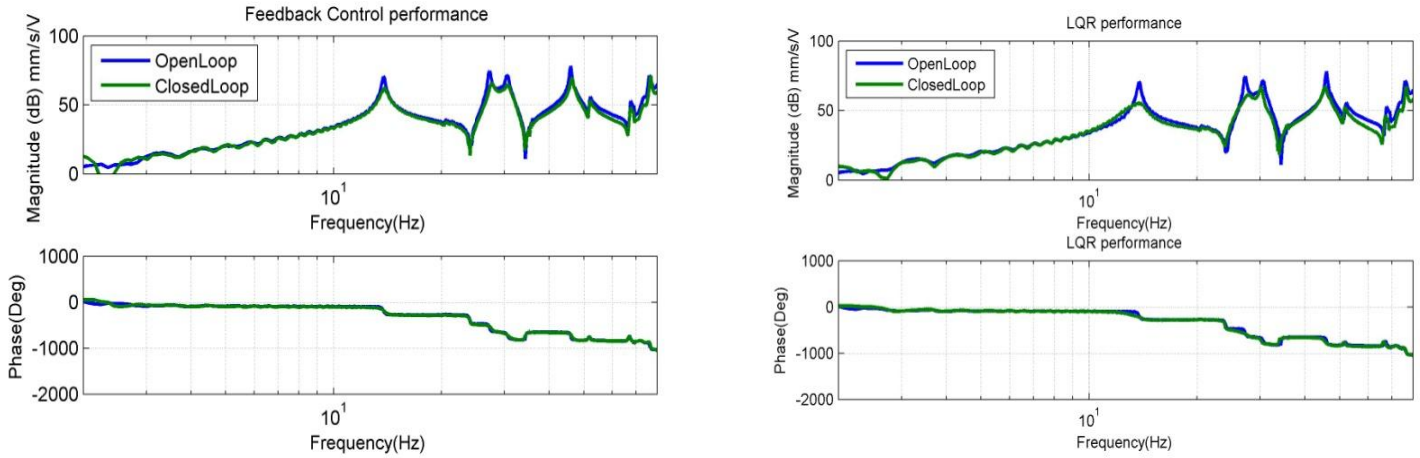

(a) (b)

Figure 4. 8 a) Control Result for Velocity Feedback Controller b) Control Result for State Feedback Controller

Figure4.8a shows the frequency response of the smart plate under proportional velocity feedback controller whereas Figure4.8b shows the frequency domain performance of the state feedback algorithm. Performance of the digitally implemented control algorithms are tabulated in Table4-2

Table 4- 2 Vibration Reduction at Resonance Frequencies of Smart Plate for Implemented Control Algorithms

	Mode 1	Mode 2	Mode 3	Mode 4
Velocity Feedback	8.6 dB	8.7 dB	6.9dB	8.5dB
LQR	14.9 dB	13 dB	5 dB	11 dB

Results presented in Table 4-2 indicates that state feedback controller performs better in vibration suppression than proportional velocity feedback controller for the first second and fourth modes. In case of the third mode, proportional velocity feedback controller manages to suppress vibration more than state feedback controller. Also broadband behavior of the smart plate for closed loop cases indicate that within the frequency span selected, implementation of the both algorithms guarantees stability.

4.1.1 Time Domain Analysis

In this subsection, time domain behavior analysis of the smart plate for digitally implemented feedback algorithms is investigated. In order to complete time domain measurements, smart plate is excited with modal frequencies of the system. Southwest patch is the disturbance source and driving signal for the southwest patch is created with NetDB. Analysis is completed for the first four modes of the controller. Those frequencies are 13.67 Hz, 27.03 Hz, 30.3 Hz and 45.6 Hz, respectively. In the beginning of the analysis controller is inactive and at the 4^{th} second controller is activated. Resultant

response of the smart plate is measured with LDV. Response of the plate is also recorded using NetDB.

4.4.2.1 First Mode Performance

The Figure4.9 shows the response of the smart plate under feedback control. Figure 4.9a indicates the response for the velocity feedback controller and Figure4.9b shows the behavior of the smart plate under state feedback control.

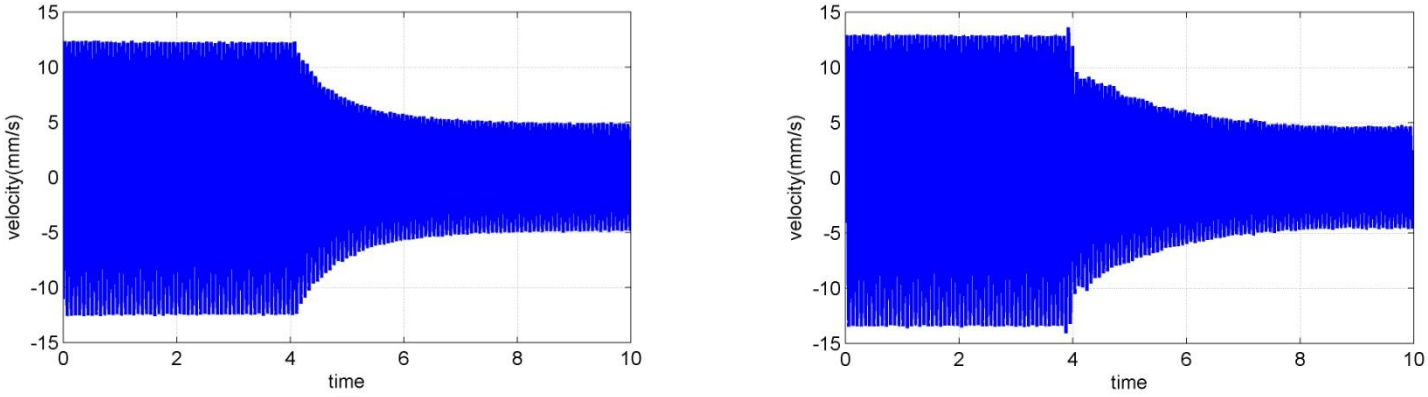

(a) (b)

Figure 4. 9 a) Control Result for Velocity Feedback Controller b) Control Result for State Feedback Controller

Controller performances for the first mode in time domain are tabulated in Table4- 3.

Table 4- 3 Time Domain Response of Smart Plate for First Mode

	Open Loop	Closed Loop
Velocity feedback	24 mm/s	11 mm/s
LQR	26 mm/s	9 mm/s

Time domain results indicate that state feedback controller performs better for the first mode of the smart plate.

4.4.2.2 Second Mode Performance

The Figure4.10 shows the response of the smart plate under feedback control. Figure4.10a indicates the response for the velocity feedback controller and Figure4.10b shows the behavior of the smart plate under state feedback control.

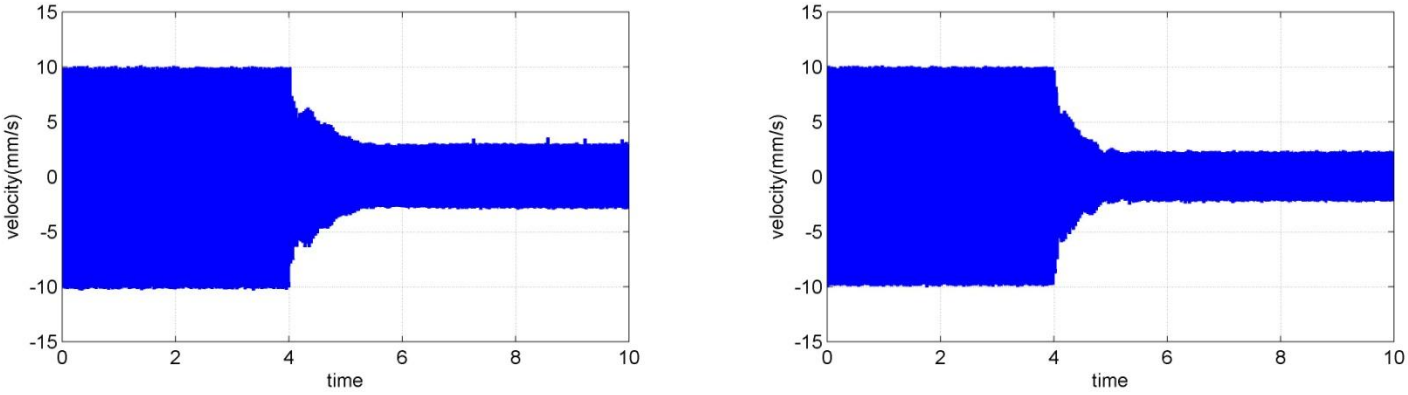

(a) (b)

Figure 4. 10 a) Control Result for Velocity Feedback Controller b) Control Result for State Feedback Controller

Controller performances for the first mode in time domain are tabulated in Table4-4.

Table 4- 4 Time Domain Response of Smart Plate for Second Mode

	Open Loop	Closed Loop
Velocity feedback	20 mm/s	6 mm/s
LQR	20 mm/s	4 mm/s

Time domain results indicate that state feedback controller performs better for the second mode of the smart plate.

4.4.2.3 Third Mode Performance

The Figure4.11 shows the response of the smart plate under feedback control. Figure4.11a indicates the response for the velocity feedback controller and Figure4.11b shows the behavior of the smart plate under state feedback control.

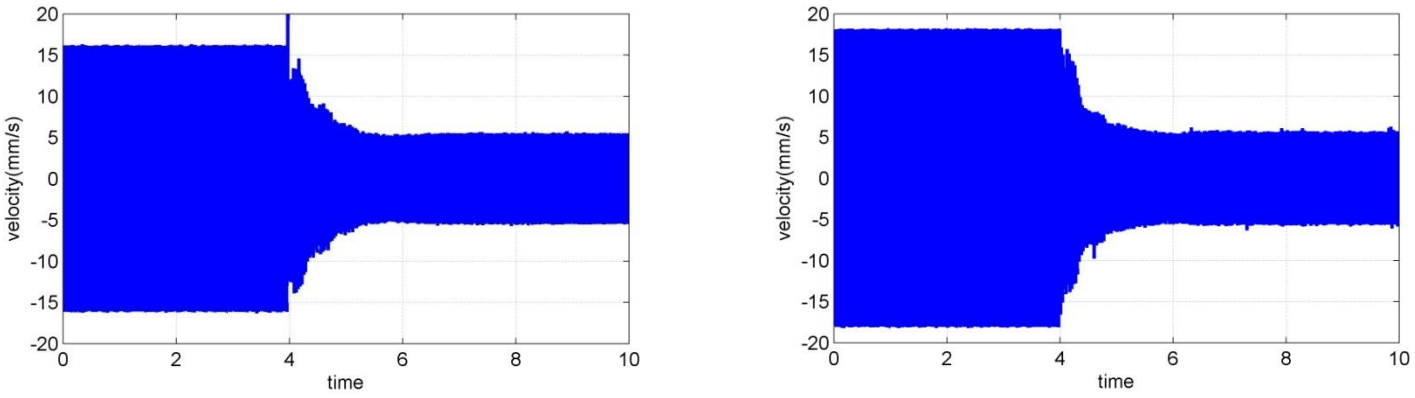

(a) (b)

Figure 4. 11 a) Control Result for Velocity Feedback Controller b) Control Result for State Feedback Controller

Controller performances for the third mode in time domain are tabulated in Table4-5.

Table 4- 5 Time Domain Response of Smart Plate for the Third Mode

	Open Loop	Closed Loop
Velocity feedback	32 mm/s	12 mm/s
LQR	36 mm/s	10 mm/s

Time domain results indicate that state feedback controller performs better for the third mode of the smart plate.

4.4.2.4 Fourth Mode Performance

The Figure4.12 shows the response of the smart plate under feedback control. Figure4.12a indicates the response

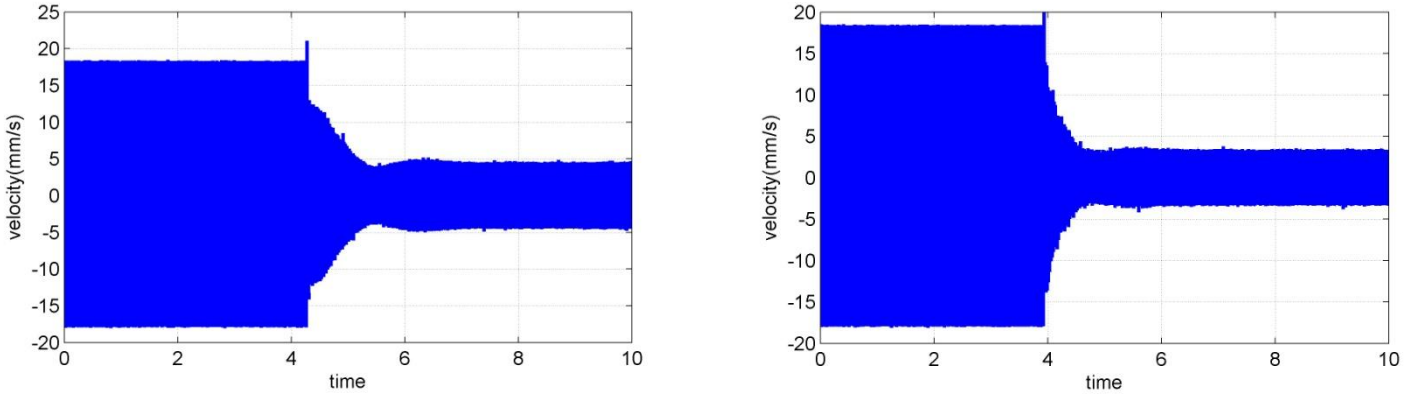

(a) (b)

Figure 4. 12 a) Control Result for Velocity Feedback Controller b) Control Result for State Feedback Controller

For the velocity feedback controller and Figure4.12b shows the behavior of the smart plate under state feedback control.

Controller performances for the fourth mode in time domain are tabulated in Table4-6.

Table 4- 6 Time Domain Response of Smart Plate for Fourth Mode

	Open Loop	Closed Loop
Velocity feedback	36 mm/s	10 mm/s
LQR	36 mm/s	6 mm/s

Time domain results indicate that state feedback controller performs better for the fourth mode of the smart plate.

4.5 Effect of Digital Control on Vibration Characteristics of the Smart Plate

In this section, change in the vibration characteristics of the smart plate due to application of the digital proportional velocity feedback controller and linear quadratic regulator is investigated. For proper analysis of the controllers, first proportional gain of the controller is adjusted to 1, 5 and 10 and frequency domain measurements are completed with open loop and closed loop scheme. Only changing parameter for the experiments is control gain of the proportional feedback controller.

For state feedback controller, different state weight matrixes, Q, are applied. The weight matrixes used are Q1=eye(10), Q2=10*eye(10), Q3=20*eye(10), Q_{mix}=diag[45 45 70 70 30 30 35 35 35 35]. Experimental set up for the LQR is the same with the digital proportional feedback controller. Changing parameters of the experiments are the Q matrixes only.

4.5.1 Results

In this section changes in vibration characteristics of the smart plate due to application of the controller are presented. As previously explained seven different configurations are utilized for the analysis. First three configurations are related to proportional velocity feedback controller while the other four are related with Linear Quadratic Regulator application. Effect of those configurations on the vibration characteristics of the plate is investigated for the first four modes of the smart plate. In Figure 4.13a, frequency response of the smart plate for velocity feedback and in Figure 4.13b frequency response of the smart plate for LQR controller are shown.

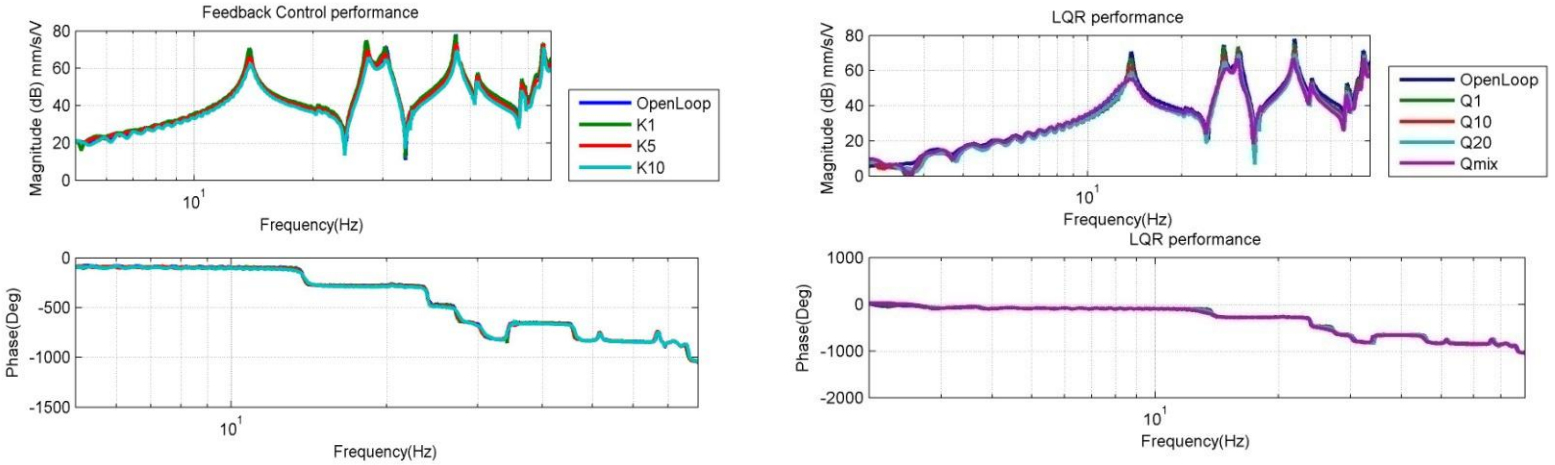

(a) (b)

Figure 4. 13 a) Frequency Domain Behavior for Velocity Feedback Controller b) Frequency Domain behavior for State Feedback Controller

In Figure 4.13a, it is obvious that as the gain increases, vibration suppression of the controller also increases. In the case of the LQR, again increasing gain yielded better results for suppression of the vibration. Manual optimization of the state gain matrix Q however changed some tendencies of the controller. Since main focus of the study is on the suppression of the first four modes, Q_{mix} yielded better results for those modes than any other gain matrix. But in the higher frequencies Q_{mix} deteriorates the suppression of the vibration in comparison to lower weight matrix. In Figure4.14, amount of the vibration suppression and modal frequency shifts due to application of the controller are shown.

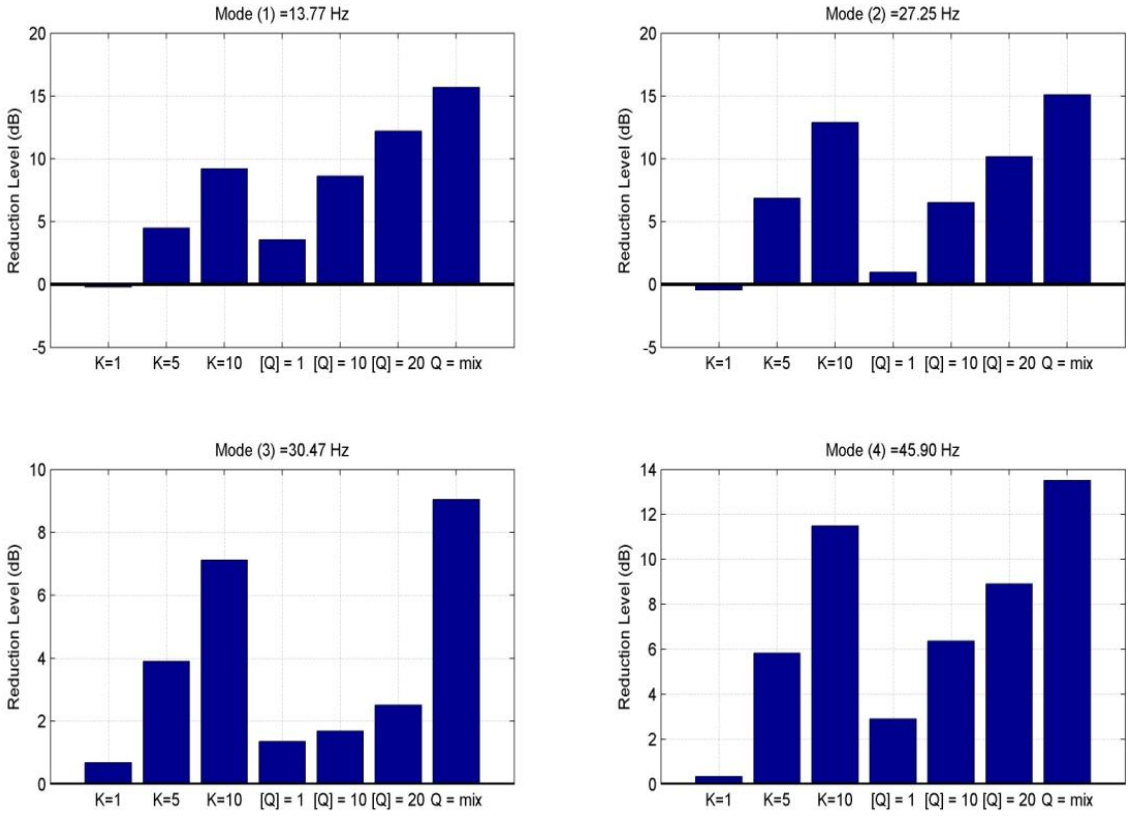

Figure 4. 14 Vibration Reduction Level of Smart Plate for Different Proportional Gains and State Feedback Controller Weight

Vibration reduction level analysis of different controller applications indicates that the best performance for the first four modes of the smart plate is achieved with optimized weight matrix Qmix. Best performance of the feedback controller is achieved with gain of 10. For lower gain analysis of the proportional velocity feedback controller, when gain of the controller is adjusted to 1, for the first and second mode, the controller is not very

efficient in suppressing the vibration and even increases the magnitude of the response. Results of the analysis showed that the LQR designed for the system performs better than the proportional velocity feedback algorithm. Even when the Q=20*eye(10) and Q=10*eye(10) LQR yields better results for some of the vibration modes of the smart plate.

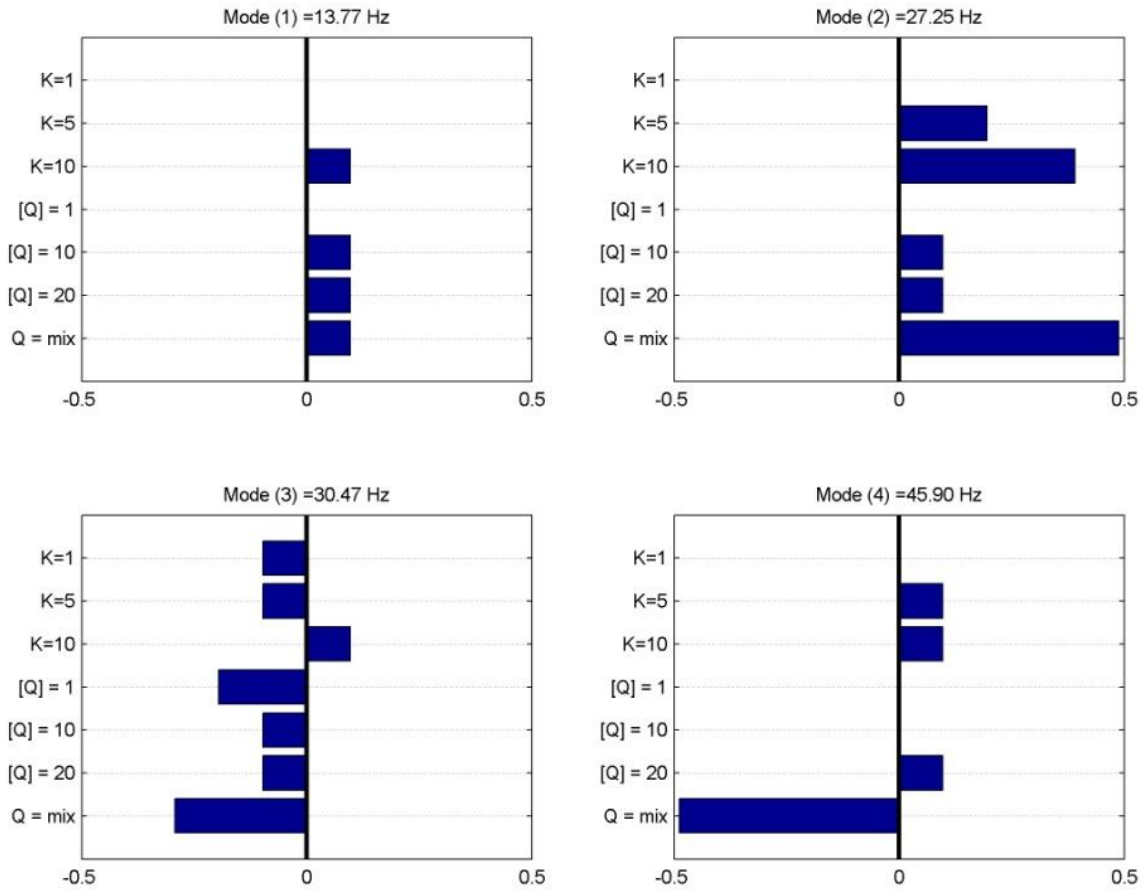

Figure 4. 15 Frequency Shifts of the Smart Plate due to Controller Implementation

Frequency behavior change of the smart plate for controller implementation is tabulated in Figure 4.15 Overall inclination of the modal frequencies is to increase when

the controller is activated. In third mode, change in the vibration characteristics is obvious since controller creates tendency for modal frequency to decrease. The most obvious frequency shifts occur for the case of the Q_{mix}.

Such changes are due to change in the damping of the structure because of the introduction of controller. LQR control relates the modes to states utilizing a model and change of the amount of the shifts and the direction of the shifts are due to state feedback matrix. State feedback matrix of the LQR adjusts output differently for modes related to each state so different damping behavior for each mode is expected. In the case of velocity feedback control, although damping is increased tendency of the controller is to decrease magnitude of the vibration at resonance frequencies. In proportional feedback control frequency shifts are not that obvious since main operation frequency of the controller is identical to the smart plate.

4.6 Conclusion

In this chapter, implementation of the digital feedback controller algorithms is presented and analyzed. Two feedback algorithms, proportional velocity feedback and optimal state feedback, are applied to smart plate. Performance analysis is completed for time domain and frequency domain for closed loop and open loop cases.

Both of the algorithms are successfully implemented and for the first four modes of the smart plate vibration suppression is achieved. Furthermore, the controller implementation does not alter the stability of the higher vibration modes. Time domain and frequency domain analysis are completed to show effectiveness of the controller.

For further analysis, varying gains of proportional velocity feedback controller and varying weight matrices of optimal state feedback controller are applied to analyze effects of controller on the vibration characteristics of the smart plate. Results showed that

increasing gain and weight matrices lead to frequency shifts and magnitude decrease in the modal behavior of the smart plate.

CHAPTER 5

DISCUSSION & CONCLUSION

Suppressing vibration with externally induced excitations is a commonly used method for vibration attenuation in case of active vibration control. In this method, sensors and actuators are used to implement a controller algorithm to decrease undesired vibration. In this thesis, we designed and developed an active vibration control system to attenuate the vibration of a plate-like structure by employing surface-bonded piezoelectric patches as actuators and a collocated velocity sensor for vibration measurements. This study focuses on the comparison of two different control architectures and presents the results of vibration attenuation levels of these two methods. The main conclusions of this thesis can be summarized as follows

In chapter 2, vibration characterization of a fully clamped thin flexible plate is presented. Investigation of vibration characteristics of the fully clamped plate is completed with different piezoelectric patch configurations. Three different piezoelectric patches are bonded on the surface of the plate. Driving signal for the actuators is created with a data acquisition system and a Laser Doppler Vibrometer (LDV) is used as the sensor for the vibration measurements. Frequency domain analysis of the system is completed for different configurations of those sensor-actuator selections. Resultant behavior of the plate is investigated and analyzed separately for each configuration to determine the best locations for the sensor/actuator pairs. It was observed that northwest patch and southwest patch were effective in exciting the modes of the structure while the center patch was ineffective in exciting the second and third mode of the structure. Furthermore, although

southwest and northwest patches are capable of exciting second and third modes, response of the smart plate at the center is low in magnitude since center of the plate is nodal for those modes. Based on the results of chapter 2, the southwest patch was chosen as the disturbance actuator while the center and northwest patches are selected as the actuators for the studies conducted in Chapters 3 and 4.

In Chapter 3, an analog circuit was designed to implement proportional velocity feedback controller to suppress the vibrations of the smart plate. Two different configurations were analyzed for the system. In the first experiment, the plate was excited using southwest patch and center patch is used as the actuator to suppress the vibrations of the plate. Control gain yielding best controller performance was adjusted for the first vibration mode of the smart plate. Frequency and time domain analysis of the controller performance were performed. Effect of the controller on modal behavior of the smart plate was analyzed using three different control gains. In the second configuration, northwest patch was used as the actuator for vibration suppression while the plate was excited from the southwest location. Effect of the controller on modal behavior of the smart plate was analyzed using three different control gains. Results showed that, analog controller implementation was effective in vibration suppression up to 6dB. Also it was observed that, the modal frequencies and amplitudes of the vibrations of the plate changed as the controller gain was increased.

In Chapter 4, vibration suppression of the smart plate with a digital controller implementation was presented. For this purpose, two feedback algorithms (velocity feedback and LQR architectures) were designed and implemented. Performance of implemented algorithms was compared and changes in vibration characteristics of the smart plate due to the controller implementation were analyzed. . Results of this chapter showed that both of the controller algorithms were effective in suppressing the vibrations of the plate but the state feedback controller performed better. Proportional velocity

feedback controller attenuated vibrations of the plate at a level of 8.6dB, 8.7dB, 6.9dB and 8.5dB for first four modes, respectively. However, the state feedback controller managed to suppress vibrations of the plate at a level of 14.9dB,13dB, 5dB, and 11dB for those modes. In the time domain analysis, this observation was also confirmed. Besides the performance evaluation of those controllers, vibration characteristics of the smart plate for different controller gains and different state feedback matrices were also investigated. Results showed that the modal frequencies and the modal amplitudes of the smart plate are changed as the controller gains and state feedback matrices were increased.

As a future topic, self-sensing configuration of the piezoelectric materials can be studied. Self-sensing property of the piezoelectric materials is advantageous since in any sensor failure, piezoelectric actuators can be used as sensors. This property of the piezoelectric materials would make them more effective for commercial applications. Other controller architectures can be also studied in a future study. Robust controllers like LQG and H_∞ can be employed to suppress vibrations of the smart plate and their performance can be compared with the ones completed in this thesis.

Another future study would be to adapt the developed methodologies to a more complex structure (eg: an automotive or aircraft panel) for active vibration control. Such a demonstration would also make it possible to see the efficiency of the developed methodologies in real life applications. In addition to the unsability of the piezoelectric materials in this type applications, the issues to be addressed are power supplies, cost, system reliability and overall system integration.

As an alternative to piezoelectric materials, scientists are motivated to use dielectric elastomers in active vibration and noise control systems. Kaal and Herold[49] investigated the nonlinearities and potential usages of a dielectric elastomer actuator for dynamic applications. Jordi[50] evaluated the performance of dielectric elastomers for large-scale applications and noted that these of type of materials have certain advantages; however the

optimization studies shall be conducted for any particular applications. Meanwhile, Wei[51] studied the vibration characteristics of electrorheological (ER) elastomer sandwich beam. They presented the variation of vibration characteristics of the sandwich beam with the applied electrical field. They concluded that this behavior of ER elastomers can be useful when the variable performance is desired in engineering applications.

BIBLIOGRAPHY

1. Bailey,T. and J. E. Hubbard, *Distributed piezoelectric polymer active vibration control of a cantilever beam.* Journal of Guidance Control and Dynamics, 1985. 8: p. 605-611.
2. Luis,J. and E.F Crawley, *Use of piezoelectric actuators as elements of intelligent structures.* AIAA Journal, 1987. 25: p. 1373-1385.
3. Ro, J. and A. Baz, *Control of sound radiation from a plate into an acoustic cavity using active constrained layer damping.* Smart Materials and Structures, 1999. 8(3): p. 292.
4. Rao, S.S. and M. Sunar, *Piezoelectricity and Its Use in Disturbance Sensing and Control of Flexible Structures: A Survey.* Applied Mechanics Reviews, 1994. 47(4): p. 113-123.
5. Loewy, R.G., *Recent developments in smart structures with aeronautical applications.* Smart Materials and Structures, 1997. 6(5): p. R11-R42.
6. Chee, C.Y.K., L. Tong, and G.P. Steven, *A Review on the Modelling of Piezoelectric Sensors and Actuators Incorporated in Intelligent Structures.* Journal of Intelligent Material Systems and Structures, 1998. 9(1): p. 3-19.
7. Alkhatib, R. and M.F. Golnaraghi, *Active Structural Vibration Control: A Review.* The Shock and Vibration Digest, 2003. 35(5): p. 367–383.
8. Gupta, V., M. Sharma, and N. Thakur, *Optimization Criteria for Optimal Placement of Piezoelectric Sensors and Actuators on a Smart Structure: A Technical Review.* Journal of Intelligent Material Systems and Structures, 2010. 21(12): p. 1227-1243.

9. Iorga, L., H. Baruh, and I. Ursu, *A Review of H_∞ Robust Control of Piezoelectric Smart Structures.* Applied Mechanics Reviews, 2008. 61(4): p. 040802.

10. Chopra, I., *Review of state of art of smart structures and integrated systems.* AIAA Journal, 2002. 40: p. 2145-2187.

11. Hanselka, H., *Adaptronics as a key technology for intelligent lightweight structures.* Advanced Engineering Materials, 2001. 3: p. 205-215.

12. Trindade, M.A., *Experimental analysis of active-passive vibration control using viscoelastic materials and extension and shear piezoelectric actuators.* Journal of Vibration and Control, 2011. 17(6): p. 917-929.

13. Hurlebaus, S. and L. Gaul, *Smart structure dynamics.* Mechanical Systems and Signal Processing, 2006. 20(2): p. 255 - 281.

14. Fakhari, V. and A. Ohadi, *Nonlinear vibration control of functionally graded plate with piezoelectric layers in thermal environment.* Journal of Vibration and Control, 2011. 17(3): p. 449-469.

15. Okumura, H., R. Emi, and A. Sano. *Adaptive Two degree-of-freedom Vibration Control for Flexible Plate with Piezoelectric Patches*. in *2008 Proceedings of SICE Annual Conference, Vols 1-7*. 2008.

16. Ryall, T. *Two considerations for the design of a robust optimal smart structure where control energy is expensive*. in *Smart Structures and Devices* 2001.

17. Ram, Y.M. and D.J. Inman, *Optimal Control for Vibrating System.* Mechanical Systems and Signal Processing, 1999. 13(6): p. 879 - 892.

18. Sebastijanovic, N., T. Ma, and H.T.Y. Yang, *Panel flutter detection and control using eigenvector orientation and piezoelectric layers.* AIAA JOURNAL, 2007. 45(1): p. 118-127.

19. Lim, Y., et al., *Finite element simulation of smart structures using an optimal output feedback controller for vibration and noise control.* Smart Materials & Structures, 1999. 8(3): p. 324-337.

20. Chomette, B., et al., *Damage reduction of on-board structures using piezoelectric components and active modal control-Application to a printed circuit board.* Mechanical Systems and Signal Processing, 2010. 24(2): p. 352-364.

21. Hwang, J., et al., *Robust LQG control of an all-clamped thin plate with piezoelectric actuators/sensors.* IEEE-ASME Transactions on Mechatronics}, 1997. 2(3): p. 205-212.

22. Sanda, T. and K. Takahashi. *Flutter and vibration control of aluminum plate wing by piezoceramic actuators*. in *SMART STRUCTURES AND MATERIALS 1998: SMART STRUCTURES AND INTEGRATED SYSTEMS, PTS 1 AND 2*. 1998.

23. Ohsumi, A., T. Inomata, and J. Sawada. *Modeling and control of elastic plates and cylindrical shells*. in *SICE 2003 ANNUAL CONFERENCE, VOLS 1-3*. 2003.

24. Song, C., et al., *Active vibration control for structural-acoustic coupling system of a 3-D vehicle cabin model.* Journal of Sound and Vibration, 2003. 267(4): p. 851-865.

25. Strassberger, M. and H. Waller, *Active noise reduction by structural control using piezo-electric actuators.* Mechatronics, 2000. 10(8): p. 851-868.

26. Yasin, M.Y., N. Ahmad, and M.N. Alam, *Finite element analysis of actively controlled smart plate with patched actuators and sensors.* Latin American Journal of Solids and Structures, 2010. 7(3): p. 227-247.

27. Jiang, J.P. and D.X. Li, *Decentralized Robust Vibration Control of Smart Structures with Parameter Uncertainties.* Journal of Intelligent Material Ssystems and Structures, 2011. 22(2): p. 137-147.

28. Bayard, D.S. and R.Y. Chiang, *Identification, uncertainty characterization and robust control synthesis applied to large flexible structures control.* International Journal of Robust and Nonlinear Control, 1998. 8(2): p. 97-112.

29. Fernando J. O. Moreira, J.R.d.F.A. and D.J. Inman, *Design of a Reduced-Order H_∞ Controller for Smart Structure Satellite Applications.* Philosophical Transactions: Mathematical, Physical and Engineering Sciences, 2001. 359(1788): p. 2251-2269.

30. Larson, C., et al. *Piezoceramic active vibration suppression control system development for the B-1B aircraft*. in *INDUSTRIAL AND COMMERCIAL APPLICATIONS OF SMART STRUCTURES TECHNOLOGIES - SMART STRUCTURES AND MATERIALS 1998*. 1998.

31. Liu, T., H. Hua, and Z. Zhang, *Robust control of plate vibration via active constrained layer damping.* Thin-Walled Structures, 2004. 42(3): p. 427-448.

32. Zhang, W., J. Qiu, and J. Tani, *Robust vibration control of a plate using self-sensing actuators of piezoelectric patches.* Journal of Intelligent Material Systems and Structures, 2004. 15(12): p. 923-931.

33. Preumont, A., *Vibration control of active structures: an introduction*. Solid mechanics and its applications. 2002: Kluwer Academic Publishers.

34. Aoki, Y., P. Gardonio, and S.J. Elliott, *Modelling of a piezoceramic patch actuator for velocity feedback control.* Smart Materials and Structures, 2008. 17(1): p. 015052.

35. Caruso, G., S. Galeani, and L. Menini, *Active vibration control of an elastic plate using multiple piezoelectric sensors and actuators.* Simulation Modelling Practice and Theory, 2003. 11(5-6): p. 403-419.

36. Chellabi, A., Stepanenko Y. and S. Dost, *Direct Optimal Vibration Control of a Piezoelastic Plate.* Journal of Vibration and Control, 2009. 15(7): p. 1093-1118.

37. Dong, X.-J., G. Meng, and J.-C. Peng, *Vibration control of piezoelectric smart structures based on system identification technique: Numerical simulation and experimental study.* Journal of Sound and Vibration, 2006. 297(3-5): p. 680-693.

38. Han, J., J. Tani, and J. Qiu, *Active flutter suppression of a lifting surface using piezoelectric actuation and modern control theory.* Journal of Sound and Vibration, 2006. 291(3-5): p. 706-722.

39. Hu, Y. and A. Ng, *Active robust vibration control of flexible structures.* Journal of Sound and Vibration, 2005. 288(1-2): p. 43-56.

40. P876.A12, *http://www.physikinstrumente.com/en/products/prspecs.php?sortnr=101790*. 2011 [cited 2011 Aug 30].

41. PDV-100. *http://www.polytec.com/us/products/vibration-sensors/single-point-vibrometers/complete-systems/pdv-100-portable-digital-vibrometer/*. 2011 [cited 2011 Aug 30].

42. NetDB. *http://www.01db-metravib.com/nvh-instruments.477/pro-120-real-time-analyser-4-channels-netdb-daq-solution.511/?L=1*. 2011 [cited 2011 Aug 31].

43. E413.D2. *http://www.physikinstrumente.com/en/products/prdetail.php?sortnr=602050*. 2011 [cited 2011 Aug 30].

44. Gardonio, P., E. Bianchi, and S.J. Elliott, *Smart panel with multiple decentralized units for the control of sound transmission. Part I: theoretical predictions.* Journal of Sound and Vibration, 2004. 274(1-2): p. 163-192.

45. Kirk, D.E., *Optimal control theory: an introduction*. Dover books on engineering. 2004: Dover Publications.

46. Dorf, R.C. and R.H. Bishop, *Modern control systems*. 2008: Pearson Prentice Hall.

47. Bemporad, A., *State estimation and linear observers*, in *Lecture notes of Automatic Control I*. Academic Year 2010-2011, University of Trento.

48. 6229, N.-P. *http://sine.ni.com/nips/cds/view/p/lang/en/nid/14136*. 2011 [cited 2011 August 31].

49. Kaal, W. and S. Herold, *Electroactive Polymer Actuators in Dynamic Applications.* IEEE ASME Trans Mechatron, 2011. 16(1): p. 24-32.

50. Jordi, C. and et al., *Performance evaluation of cutting-edge dielectric elastomers for large-scale actuator applications.* Smart Materials and Structures, 2011. 20(7): p. 075003.

51. Wei, K. and et al., *Vibration characteristics of electrorheological elastomer sandwich beams.* Smart Materials and Structures, 2011. 20(5): p. 055012.